

Presented at the 21st Sagamore Army  
Materials Research Conference on  
Advances in Deformation Processing,  
Raquette Lake, New York, Aug. 13-16,  
1974

LBL-2775 *c. 2*

THE ROLE OF DEFORMATION INDUCED PHASE  
TRANSFORMATIONS IN THE PLASTICITY OF SOME  
IRON-BASE ALLOYS

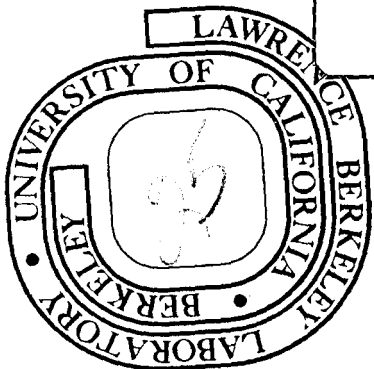
V. F. Zackay, M. D. Bhandarkar, and E. R. Parker

August, 1974

Prepared for the U. S. Atomic Energy Commission  
under Contract W-7405-ENG-48

TWO-WEEK LOAN COPY.

*This is a Library Circulating Copy  
which may be borrowed for two weeks.  
For a personal retention copy, call  
Tech. Info. Division, Ext. 5545*



LBL-2775 *c. 2*

## **DISCLAIMER**

This document was prepared as an account of work sponsored by the United States Government. While this document is believed to contain correct information, neither the United States Government nor any agency thereof, nor the Regents of the University of California, nor any of their employees, makes any warranty, express or implied, or assumes any legal responsibility for the accuracy, completeness, or usefulness of any information, apparatus, product, or process disclosed, or represents that its use would not infringe privately owned rights. Reference herein to any specific commercial product, process, or service by its trade name, trademark, manufacturer, or otherwise, does not necessarily constitute or imply its endorsement, recommendation, or favoring by the United States Government or any agency thereof, or the Regents of the University of California. The views and opinions of authors expressed herein do not necessarily state or reflect those of the United States Government or any agency thereof or the Regents of the University of California.

THE ROLE OF DEFORMATION INDUCED PHASE TRANSFORMATIONS  
IN THE PLASTICITY OF SOME IRON-BASE ALLOYS

V. F. ZACKAY\*, M. D. BHANDARKAR†, AND E. R. PARKER\*  
Inorganic Materials Research Division, Lawrence Berkeley Laboratory and  
Department of Materials Science and Engineering, College of Engineering;  
University of California, Berkeley, California 94720

## ABSTRACT

Microstructural changes in alloys can be induced by phase transformations. While many phase transformations are thermally activated, some are not. An important example of the non-thermally activated type is the deformation induced phase transformation. Deformation induced phase transformations are known to cause unusual changes in the mechanical properties of ferrous and non-ferrous alloys. In the past several years it has been shown that this type of transformation can considerably enhance the mechanical properties of high strength austenitic alloys--these alloys are now known as "TRIP" steels. Useful combinations of toughness, strength, and ductility can be obtained in these steels by control of the composition and the processing. TRIP steels are thermomechanically processed in the austenitic state. During this thermo-mechanical processing, changes occur in both chemistry and substructure, and these alter the stability of austenite with respect to deformation during subsequent mechanical testing. The present paper discusses the several compositional, processing, and testing variables that influence this austenite stability. It is shown that the strength, ductility, stress-strain behavior, fracture toughness, fatigue properties, and corrosion resistance of TRIP steels

---

\*V. F. Zackay and E. R. Parker are Professors of Metallurgy, †M. D. Bhandarkar, formerly Post Doctoral Research Metallurgist, Lawrence Berkeley Laboratory, Berkeley, California, is now with Materials Research Branch, Materials Division, NASA Langley Research Center, Hampton, Virginia 23665.

are strongly affected by austenite stability. The considerations involved in designing TRIP steels, their limitations, and some of the steps that have been taken to overcome these limitations, are reviewed. Recent studies are described in which attempts were made to incorporate the TRIP phenomenon in other classes of steels. These include non-nickel cryogenic steels and low and medium alloy quenched and tempered ultra high strength steels.

## INTRODUCTION

The elastic and plastic deformation of structural alloys does not, for the most part, entail a change of crystal structure. Although alterations in grain shape, dislocation density, and dislocation configuration may occur, the crystal structure usually remains the same; this is especially so at room temperature and below. At higher temperatures diffusion becomes possible and thermally activated phase transformations may take place. There is another class of phase transformations, the so-called martensitic type, which is known to occur without diffusion over a wide range of temperatures. This transformation can be initiated either by continuous cooling or heating, or by stress or strain.

The nature of the diffusionless austenite to martensite transformation in steels and its influence on the mechanical properties of steels have been the subjects of active research for many years. It has been recognized that under the influence of mechanical stresses and strains this transformation can occur at temperatures above the  $M_s$  (the temperature at which martensite formation first occurs on cooling a steel). Scheil observed (in an Fe-29%Ni alloy) that the amount of strain induced martensite increased with the degree of cold working and decreased with increasing deformation temperature [1]. Above a certain temperature defined as the  $M_d$ , no martensite could form from austenite as a result of deformation alone. Scheil suggested that at temperatures near the  $M_s$ , a critical resolved shear stress was required for initiation of the austenite to martensite transformation. At temperatures below the  $M_s$ , the austenite lattice becomes thermodynamically unstable and spontaneously shears to a martensitic structure without the

application of stress or strain. At temperatures sufficiently above the  $M_s$ , i.e., just above the  $M_d$ , the critical resolved shear stress for the initiation of martensite exceeds that for slip in austenite, and plastic flow supersedes the transformation.

Following the early studies of Scheil, several investigators extended theoretical analyses to account for the influence of applied stress on martensite transformation [2-6]. Cohen and his colleagues developed the reaction path theory [7,8] in which it was postulated that regions of localized strain exist in austenite and provide part of the activation energy for the martensite nucleation process. In these regions, which are called strain embryos, atoms were visualized as being displaced part way along the path to their ultimate positions in martensite. Applied stress or strain provided the additional energy that was needed to cause the growth of the strain embryos to form critical nuclei.

During the last two decades, the deformation induced austenite to martensite transformation has been studied in great detail using several iron-base alloys including the austenitic stainless steels [9-33]. These studies can be broadly divided into two types: (1) basic studies that deal with the thermodynamics, crystallography and morphology of strain induced martensite, and (2) applied studies that consider the influence of the deformation induced austenite to martensite transformation on mechanical properties. It has been shown that chemical composition and testing conditions (temperature, strain rate, etc.) affect the martensite habit plane and morphology as well as the mechanical properties such as the strain hardening rate and the elongation to fracture. Also, it has been shown that austenite can transform

into three types of martensite, namely, the bcc and the bct  $\alpha'$  martensites, and the hexagonal  $\epsilon$  martensite.

Recently, Zackay et al[34] utilized the knowledge available on the beneficial influence of the deformation induced austenite to martensite transformation to develop a new class of ultra high strength metastable austenitic steels. These newer steels were named TRIP steels (TRIP is an acronym for Transformation Induced Plasticity). The chemical composition of these steels was balanced in such a way that they were austenitic at room temperature. An important step in processing was the prior deformation of austenite (hereafter abbreviated as PDA). The primary purpose of this deformation was to raise the yield strength to 200,000 psi or above. To achieve this objective, a large amount of deformation (70 to 80% reduction in thickness) at a temperature above the  $M_d$  temperature was required. After final processing, TRIP steels are austenitic. However, when a stress or strain is applied at temperatures below the  $M_d$ , they transform to martensite. In a tensile specimen, martensite formation during testing delays necking and results in a large elongation to fracture. At yield strengths exceeding 200,000 psi elongations as high as 50% are often observed.

In TRIP steels, the stability of the austenite with respect to strain (or stress) has a significant influence on strength, ductility, work hardening rate, fracture toughness, and low cycle fatigue behavior. Gerberich et al[35] formulated an austenite stability criterion that took into account variations in chemical composition, processing, and testing. This single index of austenite stability was designated as the "stability coefficient". The relationship between the stability coefficient and mechanical properties was

studied by Gerberich et al[35] and Bhandarkar et al[36]. In the sections that follow, their conclusions and the results of several other investigators are reviewed.

The severe limitations of TRIP steels in processing and fabrication preclude their widespread application. This is unfortunate as the combinations of properties attainable cannot be duplicated in any other class of alloys. Two approaches to the solution of this dilemma are suggested: (1) modifications of processing procedures to lower the demand on equipment required in the thermomechanical working step, and (2) the design of alloys having the TRIP phenomenon, but not requiring thermomechanical working.

## TRIP STEELS

### INFLUENCE OF PROCESSING TEMPERATURE ON TENSILE PROPERTIES

The several microstructural changes that occur during processing TRIP steels can be of two types: (1) chemical changes involving carbide precipitation and carbon atom segregation, and (2) structural changes involving alterations in crystal structure, grain structure, and defect structure. Microstructural changes alter austenite stability and affect the mechanical properties of TRIP steels. In order to study the role of processing on stability and mechanical properties, it is desirable to identify and, where possible, isolate the types of microstructural changes that occur during processing. Extensive investigations of Bhandarkar et al[36] established the role of processing in altering microstructure, stability, and mechanical properties. They studied steels of widely differing compositions and processing histories, including (a) a series of carbonless iron-nickel alloys of varying austenite stability, (b) a steel containing nickel and carbon

without a strong carbide former, and (c) a series of steels of varying stability containing nickel, carbon, chromium, and manganese. The compositions of these steels are given in Table I. The weaker carbonless Fe-Ni alloys were studied because the changes induced by processing were limited to those of structure. Chemical as well as structural changes were induced by processing in the Fe-Ni-C and the Fe-Ni-Cr-Mn-C steels. In the latter, the effect of a moderately strong carbide former (chromium) was studied. A large part of the present discussion is taken from the work of Bhandarkar et al cited above.

All alloys were austenitized, brine quenched, and then given the prior deformation by rolling (PDA) before testing. The amount of transformation that occurred during testing was determined quantitatively by measuring the saturation magnetization of specimens before and during testing at various temperatures. The readings were converted to volume percentage of martensite, with corrections being made for the influence of the alloying elements [37-39]. This method could not be used for the ferromagnetic carbonless high nickel alloys. For these alloys the volume percent martensite was estimated by metallography.

The approximate  $M_s$  and  $M_d$  temperatures for all alloys were determined either by metallographic, magnetic, or electrical resistivity techniques and are listed in Table II. Their thermomechanical history of each alloy is also indicated in the Table; as indicated, transformation temperatures sometimes change with variations in processing. (Additional details on the experimental procedure are contained in the original papers cited in the bibliography.)

#### Carbonless Iron-Nickel Alloys

In the absence of carbon, the only changes that were induced by the PDA in metastable austenite were those of substructure and grain structure. The

Fe-Ni alloy 38N, whose  $M_s$  and  $M_d$  were below the lowest PDA temperature ( $-120^\circ\text{C}$ ), was first investigated. The mechanical properties of this stable alloy were established to provide a basis for comparison with the more complex and less stable alloys subsequently investigated.

The effects of the PDA temperature on the room temperature and  $-196^\circ\text{C}$  yield strengths of alloy 38N are shown in Figure 1(a)[36]. Linear variations of the yield strengths with PDA temperature were observed; the effect of varying the PDA temperature was small. Characteristically, the room temperature elongation values were small and the rates of work hardening were low.

The effect of the PDA temperature on the carbon-free alloy 34N, which was stable above room temperature but unstable at cryogenic temperatures, was determined next. The yield strengths are shown in Figure 1(b) as a function of the PDA temperature[36]. The yield strengths rose rapidly below the  $M_d$ , which was found to be between  $10^\circ$  and  $22^\circ\text{C}$ . The  $M_s$  was about  $-85^\circ\text{C}$ . Above the  $M_d$ , the variation of the yield strengths with the PDA temperature was nearly identical to that observed for the stable alloy 38N. Martensite was produced during the rolling operations below the  $M_d$ . Its presence raised the room temperature yield strength. The martensite (both athermal and deformation induced) produced during processing is clearly visible in Figure 2[36]. The before-testing microstructure of the alloy rolled at  $-120^\circ\text{C}$  is shown in Figure 2(a) and the athermal martensite produced during cooling to the test temperature after rolling above the  $M_d$  is shown in Figure 2(b).

The behavior of the less stable alloy 34N was significantly different from that of alloy 38N with respect to testing temperature, as can be seen by

comparing Figure 1(b) with Figure 1(a). With a change in test temperature from 22° to -196°C there was a sharp drop in the yield strength (about 22%) of alloy 34N. The decrease in yield strength at the lower test temperature was observed above a PDA temperature of about -100°C; at lower PDA temperatures the alloy was stronger at -196°C than it was at 22°C. A drop in yield strength at low test temperatures has been observed by several other investigators. This phenomenon has been attributed to the stress induced formation of martensite[1-4,10,11,16,18,21,24,28,40,41]. Yielding occurs as a consequence of the phase transformation when the critical stress for transformation is less than that required for the initiation of slip in austenite. Certain features of the engineering stress-strain curves of specimens tested at both room and cryogenic temperatures support this view as described below.

Typical stress-strain curves of specimens tested at both 22° and -196°C for alloy 34N, deformed 70% at a PDA temperature of 450°C, are shown in Figure 3[36]. The stress-strain curve of the specimen tested at room temperature was characteristic of that of a stable cold-worked austenitic steel, i.e., a high yield strength, a low rate of work hardening, and an elongation of about 10%. The absence of serrations in the stress-strain curves and the low work hardening rate were consistent with metallographic observations which revealed that no martensite was present in the specimens after testing. Stress-strain curves of specimens deformed at all PDA temperatures above  $M_d$  and tested at room temperature were similar to the 22°C curve shown in Figure 3.

The stress-strain curve for the specimen tested at -196°C was different in several respects. As shown in Figure 3, yielding of the austenite occurred at a lower stress than that observed at 22°C. The rate of work hardening was

high, and the elongation was nearly twice that of the specimen tested at room temperature. The low elastic limit observed in the test at  $-196^{\circ}\text{C}$  was attributed to the formation of martensite nucleated by local stresses at loads below the elastic limit of stable austenite at the test temperature. The high rate of strain hardening in the plastic strain range is strong evidence of strain induced martensite formation. Thus both stress induced and strain induced martensite formed in this specimen during the test. Also, a metallographic examination of the unstrained end of the test specimen revealed that about 70% of athermal martensite was present prior to tensile testing (Figure 2(b)). After testing, the alloy in the gage length was almost completely martensitic. Stress-strain curves of specimens deformed at all PDA temperatures above the  $M_d$  and tested at  $-196^{\circ}\text{C}$  were similar to the one shown in Figure 3.

The mechanical properties observed can be explained if the deformation mechanisms include strains due to the formation of stress induced martensite. In recent years a number of investigators have emphasized the importance of this mechanism of plastic flow in metastable austenitic steels, especially at temperatures near the  $M_s$ . Angel[10], in particular, made detailed studies of the yield behavior of annealed metastable steels at temperatures ranging from above the  $M_d$  to below the  $M_s$ . Some of his conclusions were as follows: at temperatures above the  $M_d$  the yielding is entirely by slip of the austenite; below the  $M_d$  and above the  $M_s$ , two other mechanisms of flow are likely to be operative, either singly or together, viz., the strain induced and the stress induced modes of the transformation of austenite to martensite; and, finally, below the  $M_s$  the stress induced mode of the transformation is dominant.

Angel stressed that between the  $M_d$  and the  $M_s$ , the two modes of yielding mentioned above were competitive, the dominant one being determined by the test temperature. The strain induced mode is favored near the  $M_d$  and the stress induced mode is favored near the  $M_s$ .

Fahr[41] has shown in a recent study that certain metastable austenitic steels of low stability have low yield strengths and high rates of work hardening. He concluded that these properties were characteristic of alloys in which the formation of martensite was stress induced. In unpublished work, Fahr observed yield-to-tensile strength ratios as low as one-quarter[40]. As illustrated in Figure 3, the total elongation of a non-carbon containing Fe-Ni alloy undergoing a stress induced transformation may be nearly twice that of a similar, but stable, alloy. It will be shown in a later section, however, that metastable steels containing carbon may have low ductility because of the brittleness of the stress induced martensite. Thermomechanical treatments which tend to stabilize austenite favor the strain induced transformation, while those which destabilize the austenite favor the stress induced mode.

The variation of the yield strength with the PDA temperature for alloy 34N is shown for test temperatures of  $-78^\circ\text{C}$  and  $22^\circ\text{C}$  in Figure 4[36]. The mechanical properties between the  $M_d$  (approximately  $15^\circ\text{C}$ ) and the  $M_s$  ( $-85^\circ\text{C}$ ) were consistent with the observations of Angel, namely, that either the stress induced or the strain induced, or both modes of the transformation may occur when tensile tests are made in this temperature range. Both modes did occur in specimens having PDA temperatures of  $25^\circ$  and  $100^\circ\text{C}$  when they were tested at  $-78^\circ\text{C}$  (Figure 4). Metallographic studies of the specimen having a PDA temperature of  $25^\circ\text{C}$  confirmed the fact that no martensite was present before testing, but that a large amount existed after testing.

As shown in Figure 4, the  $-78^{\circ}\text{C}$  yield strength increased with increasing PDA temperature, rising to a value greater than that measured at room temperature. This behavior showed that processing at higher PDA temperatures stabilized the austenite, thereby favoring the strain induced over the stress induced transformation. The principal features of the stress-strain curves for alloy 34N are shown in Figure 5[36]. As a consequence of the stability change, the extent of the Lüders strain increased with the PDA temperature, the rate of strain hardening decreased, and the total elongation became larger.

A direct measurement of the stability change produced by varying the PDA temperature was made by determining the  $M_d$  for two extreme PDA temperatures, viz.,  $25^{\circ}$  and  $450^{\circ}\text{C}$ . The  $M_d$  temperatures, estimated by means of metallographic and X-ray diffraction techniques of the strained tensile specimens, were found to differ by about ten degrees; the specimen with the PDA temperature of  $450^{\circ}\text{C}$  had the lower  $M_d$ . This result supported the view that the stability, the mode of transformation, and the mechanical properties of a carbonless austenitic alloy were changed by thermomechanical processing. In carbon containing steels chemical as well as structural changes were produced by processing with similar, but larger, effects on stability and mechanical properties as shown in the following section.

#### Iron-Nickel-Carbon and Iron-Nickel-Chromium-Manganese-Carbon Steels

A series of steels was prepared to investigate the interrelationships between processing, austenite stability, and mechanical properties. The principal variables were the composition of the steel and the PDA temperature. The amount of the deformation was held constant.

The amounts of nickel, manganese and carbon in the first steel of this series, CN28, were adjusted so that the  $M_d$  was in the same temperature range as that of the carbon-free alloy 34N. The nickel contents of the remaining steels of the series were varied to cause systematic changes in austenite stability, as shown in Table II. The levels of carbon, manganese, and chromium were maintained essentially constant. The relation between structure and properties of the iron-nickel-carbon steel for several processing and testing conditions are discussed first.

The variation of yield strength with the PDA temperature for steel CN28 (70% deformation) is shown in Figure 6 for two test temperatures [36]. The  $M_s$  of this steel after processing was estimated to be  $-68^\circ\text{C}$  and the  $M_d$  was estimated to be about  $25^\circ\text{C}$ . At PDA temperatures below the  $M_d$ , strain induced martensite was formed. The high yield strengths obtained at the lower PDA temperatures reflected the duplex nature of the microstructure. The behavior was similar to that of alloy 34N, except that the overall strength level was higher because of the greater hardness of the martensite.

For PDA temperatures above the  $M_d$ , the yield strength varied in a different manner from that of the carbonless iron-nickel alloys, as can be seen by comparing Figure 1(b) with Figure 6. A broad maximum was found between  $200^\circ$  and  $300^\circ\text{C}$  for the carbon containing steel CN28. A similar maximum was also evident at the  $-78^\circ\text{C}$  test temperature even though the strength level was almost 100,000 psi below that found at  $22^\circ\text{C}$ . The lower yield strength at the lower test temperature was attributed to the stress induced formation of martensite.

Maxima in yield strength of the kind shown in Figure 6 appeared to be unique to alloys containing carbon; they were never observed in carbon-free alloys. Yield strength maxima were obtained with steels of widely differing stabilities. The variation of the room temperature yield strength with PDA temperature for steels CN8Cr, CN12Cr, and CN21Cr (whose  $M_d$  temperatures were 150°, 22°, and -196°C respectively) are shown in Figure 7[36]. These steels were processed in a similar manner; they differed primarily in nickel content. When tested at 22°C, they exhibited maxima varying slightly from each other in height and position. Similar peaks were also found when tests were made at -78°C, as shown in Figure 8[36]. The low -78°C yield strengths of CN8Cr, the least stable steel, were due to the stress induced martensitic transformation.

Other investigators who have made elevated temperature tensile tests on annealed austenitic steels have found peaks in the yield strength vs temperatures curves, and such peaks have also been found in martensitic steels[14,42-48]. Such maxima are usually attributed to the formation of carbon atmospheres or precipitates on the dislocations. Parker and Hazlett, as well as others, have concluded that clusters and precipitates formed in this manner can lead to small but significant increases in yield strength[42,48,49].

While the combined electron microscopy, magnetic, and mechanical property evidence (see Hall et al[50], Chanani et al[51], and Bhandarkar et al[36]) was consistent with the concept that the yield strength peaks of Figures 7 and 8 resulted from chemical changes associated with the various states of aggregation of carbon in the austenite lattice, conclusive evidence that this was so is not yet available. The lower yield strengths associated with PDA temperatures above 250°C are thought to be a consequence of smaller amounts of carbon

clustering around dislocations because of the higher solubility of carbon in austenite. Conversely, at PDA temperatures below 250°C the mobility of the carbon is considered to be too low to form atmospheres in the time available during deformation.

#### INFLUENCE OF THE AMOUNT OF PRIOR DEFORMATION ON TENSILE PROPERTIES

Fahr[41] conducted an extensive investigation of the influence of the amount of prior deformation of austenite on mechanical properties. In a series of 9Cr-8Ni-2Mn steels with carbon contents ranging from 0.1 to 0.5%, Fahr varied the amount of rolling reduction, at 450°C, from 20 to 80%. In the 0.1% and 0.5%C steels the yield strength increased with increase in the amount of prior deformation, as shown in Figure 9 (adapted from [41]). From the figure, it is evident that the steel with the higher carbon content experienced a greater increase in yield strength than the steel with the lower carbon content.

A steel with a carbon content of 0.2% exhibited an unusual variation in yield strength as a function of the amount of prior deformation. The yield strength of this steel was greater for a prior deformation of 60% than for one of 80%. Fahr attributed this unusual behavior to the lower stability of the 80% deformed steel leading to a stress induced martensite transformation during testing. The lower stability presumably resulted from the greater amount of precipitation in the 80% deformed steel.

In additional experiments using a 9Cr-8Ni-3Mn-0.4C steel, Fahr observed that the yield strength increased and fracture elongation decreased as the amount of prior deformation at 450°C was raised from 20% to 60%. Both the yield strength and the elongation increased when the amount of prior

deformation was raised to 80%. These results are shown in Figure 10 (adapted from [41]).

Several conclusions can be drawn from the above results. In TRIP steels the increased dislocation density resulting from the prior deformation of austenite leads to mechanical stabilization of the austenite. The larger the amount of deformation, the greater the stabilization. When this type of stabilization is the predominant factor, increasing amounts of prior deformation result in an increase in yield strength and a decrease in elongation.

Carbide precipitation causes the removal of carbon and carbide-forming alloying elements from the austenitic matrix thus leading to a reduction in austenite stability. In high carbon steels which are highly stable prior to processing, a decrease in austenite stability due to excessive carbide precipitation, especially for high deformations and long times at temperatures during deformation, may offset the mechanical stabilization effect. This would lead to increases in both yield strength and elongation (compare the results in Figure 10 for the 9Cr-8Ni-3Mn-0.4C steel deformed 60% and 80%). However, if austenite stability prior to processing is not sufficiently high, a decrease in stability due to excessive carbide precipitation would lead to a stress induced martensitic transformation during subsequent testing. In this latter case both yield strength and elongation are lowered for increases in the amount of deformation. An example of this is shown in Figure 11 (adapted from [41]) where both the yield strength and elongation of a 9Cr-8Ni-2Mn-0.2C steel are lowered when the amount of deformation is raised from 60% to 80%.

#### CONCEPT OF STABILITY, AND STABILITY CRITERIA

In earlier sections, the changes in austenite stability (with respect to

athermal and deformation types of transformations) produced by variations in chemical composition and processing have been described in qualitative terms. There have been attempts to establish quantitative measures of stability [10,35] which are relevant to the present investigation. In the following discussion two criteria are compared using data obtained on the carbon containing steels.

Angel, in a study of austenitic 18-8 type stainless steels, found that an equation of the type

$$\ln \frac{f}{1-f} = A \ln \epsilon + k \quad (1)$$

best fitted his data [10]. In this equation,  $f = \frac{V_{\alpha}}{V_T}$  where  $V_{\alpha}$  is the volume of austenite transformed to martensite,  $V_T$  is the maximum amount of martensite that can form by plastic deformation,  $\epsilon$  is the true strain, and  $A$  and  $k$  are constants. The equation is of the log autocatalytic type proposed by Austin and Rickett [52], with the strain parameter replacing time. Gerberich et al, have reported that the volume fraction of martensite,  $V_{\alpha}$ , produced during a tensile test varies as

$$V_{\alpha} = m \epsilon^{1/2} \quad (2)$$

where  $m$  is a constant for a given set of test conditions and  $\epsilon$  is the conventional strain [35]. The value of  $m$  was obtained by plotting  $V_{\alpha}$  vs  $\epsilon^{1/2}$  and fitting the best straight line to the data. Typical experimental data for steel CN8Cr, deformed 70% at 450°C, are shown in Figure 12 for test temperatures of 22°, -78°, and -196°C [36]. Curves representing the relationships of  $V_{\alpha}$  and  $\epsilon$  suggested by Angel and Gerberich et al, are also shown in Figure 12. For the Angel criterion all calculations were based on true strain, whereas engineering strain was used for the Gerberich function. It is evident that neither criterion accurately predicted the data over the complete range of

strains. For the room temperature test, the data at low strains were in better accord with the Angel model, but at higher strains, the Gerberich formulation appeared to be superior.

Gerberich showed that the coefficient  $m$ , while approximate, was a useful index of austenite stability for TRIP steels of widely varying chemical compositions and processing histories. In these steels this coefficient can be varied from zero (completely stable) to about 3.5 (highly unstable). The value of  $m$  is zero when the test temperature is at or above the  $M_d$  temperature--the temperature above which plastic strain will not induce a transformation.

The deformation-transformation characteristics and their relationships to static and fatigue properties were studied by Weiss et al [53] for a number of TRIP steels containing 0.2%-0.03%C. Under room temperature monotonic tensile loading the TRIP steels deformed linearly to a stress maximum which was followed by a sharp "yield drop". No appreciable amount of martensite formation was detected during the linear portion, while rapid martensite formation occurred during Lüder's band formation and spreading, thus supporting the suggestion that martensite transformation was strain nucleated. The parabolic relationship between strain and volume percent martensite (equation 2) suggested by Gerberich could not be confirmed. During early stages of the deformation, martensite formation was very rapid, perhaps proportional to the square of the strain. Later, saturation developed at a martensite level and strain that seemed to be characteristic for the particular TRIP steel, test temperature, and strain rate.

## STABILITY AND TENSILE PROPERTIES

Deformation induced carbon containing martensite in highly dislocated austenite is presumably stronger than the parent phase. Deformation induced martensite ribbons distributed throughout the austenitic matrix profoundly alter ductility, strain hardening rate, tensile strength, and fracture toughness. When martensite forms during a tensile test, necking is delayed until high strains are reached. The uniform elongation and the tensile strength are increased because of the high rate of strain hardening caused by martensite "barriers" to further plastic flow.

A stability index for high strength metastable austenitic steels would permit predictions to be made of the effect of composition and processing conditions on mechanical properties. In the ensuing discussion, the Gerberich index is used as a relative measure of austenite stability in an effort to correlate the tensile properties of the steels with their composition and processing.

The influence of the stability coefficient  $m$  on the elongation to fracture for a large group of TRIP alloys of widely varying compositions, processing histories and testing temperatures is shown in Figure 13(a) (adapted from [35]). The dilatational and shear components of the austenite to martensite transformation enhance elongation and also increase the Lüders strain (i.e., the strain in the flat part of the stress-strain curve following initial yielding). The influence of the stability coefficient  $m$  on the extent of the Lüders strain for the same group of alloys is shown in Figure

13(b) (adapted from [35]). Similar correlations exist for the rate of strain hardening and the tensile strength[35].

The engineering stress-strain curves at several testing temperatures are shown in Figure 14 for the CN8Cr steel deformed 70% at 450°C[36]. The  $m$  values are also shown. The stress-strain curve obtained at 22°C exhibited a well defined Lüders strain, a low work hardening rate, and an elongation at fracture of 20% corresponding to an  $m$  value of 1.85, as shown in Figure 13(a) and (b). The relatively low rate of work hardening is a consequence of the comparatively low rate of formation of martensite with strain, as can be seen from Figure 12(a).

At the test temperature of -78°C, both the stability and the shape of the stress-strain curve are quite different, relative to those at room temperature, as can be seen in Figure 12(b) and Figure 14. The yield strength was lower by about 60,000 psi, the Lüders band was well defined, the rate of work hardening was much higher, and the elongation at fracture was about one-half of the room temperature value. These features are consistent with the change in stability as reflected by the  $m$  value, 2.37 (Figure 13). The low yield strength and the high rate of work hardening are of particular interest. These features are characteristic of an alloy undergoing a stress induced phase transformation. The large amount of martensite produced at low strains is another characteristic feature of this type of transformation. At a strain of 0.02, about half the austenite had transformed to martensite in the -78°C test. In the specimen tested at 22°C, less than 10% of the austenite had transformed for the same strain.

The stress-strain curve and transformation behavior of the specimen tested at  $-196^{\circ}\text{C}$  were similar in kind but different in detail from those observed at  $-78^{\circ}\text{C}$ . The yield strength was somewhat higher (by about 25,000 psi), a reflection of the increased strength of austenite at the lower temperature. The rate of work hardening, the extent of the Lüders strain, and the elongation to fracture were similar to those observed at  $-78^{\circ}\text{C}$ , as was the rate of formation of strain induced martensite at strains above about 0.05. The latter behavior was observed when the volume fraction of martensite vs strain curves for the two test temperatures were replotted after making a correction of 0.15 for the extra stress induced martensite that formed at  $-78^{\circ}\text{C}$ . The two curves approximately coincide, as shown in Figure 12(d). The estimated value of  $m$  is 2.37 and the Gerberich relation can be written as  $V_{\alpha} - V_0 = m\epsilon^{1/2}$ , where  $V_0$  is the volume fraction of stress induced martensite that formed just after the yield point. It is well known that the modulus and the yield strength of fcc metals increase with decreasing temperature[54,55]. The increased resistance to flow should reduce the amount of stress induced martensite. Consistent with this explanation is the fact that the flow stress is higher at  $-196^{\circ}\text{C}$  than at  $-78^{\circ}\text{C}$ , as shown in Figure 14, and the fact that the volume fraction of stress induced martensite is lower at  $-196^{\circ}\text{C}$  than at  $-78^{\circ}\text{C}$  as shown in Figure 12(b) and (c).

A correlation similar to that produced by a change in test temperature can be made by varying the stability with changes in composition or with PDA temperature. The stress-strain curves for three steels of differing nickel contents, deformed 70% at  $450^{\circ}\text{C}$  and tested at  $-78^{\circ}\text{C}$ , are shown in Figure 15 [36]. Most of the key features in these curves have been previously discussed. However, the striking difference in behavior between the completely

stable steel, CN16Cr, and the highly unstable one, CN8Cr, is worthy of note, as is the comparatively large elongation of steel CN12Cr. As Bressanelli and Moskowitz[22], Tamura et al[26], and Gerberich et al[35] have observed, maximum elongation is produced in metastable austenitic steels when martensite is produced at an optimum rate with strain. Too little martensite per unit of strain fails to prevent necking and too much results in premature failure by fracture of the brittle martensite. The relatively low  $m$  value (estimated to be between 1.0 and 1.5) indicated that for steel CN12Cr the criterion for a large elongation to fracture was met.

Changes in austenite stability can be induced by variations in the PDA temperatures, as shown earlier for both the carbonless Fe-Ni alloys and the carbon containing steels. The room temperature engineering stress-strain curves of steel CN8Cr, deformed 70% at PDA temperatures of 200° and 450°C are shown in Figure 16 (adapted from [36]). The difference in stability (as reflected by the  $m$  values) produced by varying the PDA temperature markedly influenced the shape of the stress-strain curves. The well defined (and small) Lüders strain and the high work hardening rate of the specimen deformed at 450°C (as compared with the one deformed at 200°C) reflected the decreased stability produced by the higher deformation temperature. These features are consistent with the data shown in Figure 13.

The approximate shape of the engineering stress-strain curves of TRIP steels can be predicted by the known empirical relations between the stability index  $m$  and the tensile properties[35]. The rule of mixtures is invoked to describe the mechanical behavior of austenite-martensite combinations. The austenite stability index is generally determined experimentally or it can be

calculated from the relationships between stability, composition, and processing conditions[35].

#### FRACTURE TOUGHNESS

Several investigators have suggested that a stress or strain induced phase transformation might enhance the absorption of energy and thereby increase the fracture toughness. The fracture toughness of TRIP steels has been studied from both the theoretical and experimental viewpoints[56-63]. It is clear from these studies that the toughness is dependent upon the stability, the chemical composition of the strain induced martensite, and the strain rate.

Gerberich et al showed that as a first approximation the fracture toughness  $K_{Ic}$  was proportional to  $m^{1/2}$ [62]. Room temperature plane stress fracture toughness values of almost 500,000 psi-in<sup>1/2</sup> were reported for highly unstable ( $m=2$ ) steels having yield strengths of 200,000 psi or higher; a summary of the data is shown in Figure 17[60,62]. The fracture toughness decreased with increasing amounts of carbon plus nitrogen in the steel. The effect of carbon content on the apparent  $K_{Ic}$  value at -196°C is shown in Figure 18[62]. Fractographic analysis showed that the martensite in the higher carbon steels (over 0.27%) had a tendency to fail by cleavage rather than by shear. The variation of apparent  $K_{Ic}$  values with carbon content, at -196°C, reflects this change of fracture mode.

Gerberich et al[59,62] and Antolovich and Singh[61] derived analytical expressions which include the contribution of the phase transformation to the observed fracture toughness of TRIP steels. Both groups of investigators concluded from theoretical and experimental evidence that the phase transformation was a major source of the fracture toughness of TRIP steels.

Antolovich and Singh[61] experimentally determined this contribution to be between two-thirds and three-fourths of the measured crack extension force,  $G_{Ic}$ .

When austenite transforms to martensite, there is an increase in volume of about three percent. This corresponds to a linear increase of one percent in each of three perpendicular directions. This volumetric expansion effectively cancels a large part of the triaxial stress that exists near the root of a sharp deep crack or notch. The reduction in the triaxial component of stress has a marked effect on the behavior of thick specimens, where triaxiality is a major contributor to brittle behavior[64]. As a consequence, TRIP steels exhibit an unusual variation in fracture toughness with specimen thickness. The fracture toughness of virtually all high strength alloys decreases sharply with increasing thickness. This does not appear to be the case in TRIP steels. As shown in Figure 19, the critical stress intensity factors (K), at room temperature, of both the low alloy quenched and tempered steel and the precipitation hardening stainless steel decrease with thickness more severely than that of the TRIP steel (adapted from [62]).

In Figure 20 the estimated fracture toughness of TRIP steels is compared with the toughness of commercial AISI 4340 and 18% nickel maraging steels. The superior toughness of TRIP steels is evident from the figure[65]. The data on TRIP steels were plane stress fracture toughness ( $K_c$ ) values. Test results did not meet the ASTM specified validity criteria[66] for plane strain fracture toughness  $K_{Ic}$  although several tests were performed using one inch thick specimens. The strain induced austenite to martensite transformation occurring during testing apparently relaxed the triaxiality at the crack

tip thus leading to nonvalid "plane strain" fracture toughness values.

#### BEHAVIOR UNDER CYCLIC LOADING

A large number of engineering structures are subjected to both monotonic and cyclic loads during their service life. In designing such structures proper consideration must be given not only to strength and fracture toughness, but also to fatigue properties such as the resistance to fatigue crack propagation and the number of load (or strain) reversal cycles required for failure.

Investigations of the behavior of TRIP steels under cyclic loading have not clearly established the role of austenite stability. Chanani[67] and Chanani and Antolovich[68] conducted high strain low cycle fatigue tests on polished specimens of a 9Cr-8Ni-4Mo-3Mn-3Si-0.26C TRIP steel with both austenitic and mixed austenitic-martensitic matrices. Tests were performed at room temperature (below  $M_d$ ) and at 200°C (above  $M_d$ ). In all cases the low cycle fatigue life was shown to be related to the plastic strain range by the Coffin-Manson law[69-71],

$$\epsilon_{PR} N_f^{1/2} = C \quad (3)$$

where  $\epsilon_{PR}$  is the plastic strain range,  $N_f$  is the number of cycles for failure and  $C$  is a constant. It was concluded that low cycle fatigue properties were controlled by the reduction in area and that the martensite transformation occurring during testing played only a secondary role. It is not known whether the above conclusion applies to all TRIP steels.

Studies of fatigue crack propagation in TRIP steels have been directed toward establishing the mechanism of crack growth at various applied stress intensity ranges[67,72]. The Paris-Erdogen relation[73] was used to relate

the applied stress intensity range  $\Delta K$  to  $\frac{da}{dn}$ , the incremental extension (da), for a given number of cycles (dn), of a crack of length 'a'. A fourth power dependence was found between  $\Delta K$  and  $\frac{da}{dn}$ . The results indicated that three prior deformation treatments (20 and 80% at 450°C, and 80% at 250°C) resulted in approximately the same crack growth properties in a 9Cr-8Ni-4Mo-3Mn-3Si-0.25C steel, and these properties were superior to those of the steel with a 20% PDA at 250°C. The strain induced austenite to martensite formation appeared to have a distinct beneficial effect. Fatigue fractures were characterized by striations, quasi-cleavage, and elongated dimples. The lowest crack propagation rates of the TRIP steel were slightly lower than those reported in the literature for 300-M steel, AM 355 CRT stainless steel, and PH 15-7 Mo steel, and compared favorably with those of 250 grade maraging steels[74-76]. All these steels had the same tensile strength.

In a recent report Weiss et al [53] stated the following:

"Fatigue crack growth rates were also found to be quite sensitive to austenite metastability. At room temperature and at higher temperatures below  $M_d$ , the fatigue crack growth resistance was inferior to that of a comparable ultra high strength steel. At liquid nitrogen temperature, where considerable martensite formation occurs, even at low plastic strains, the fatigue crack growth resistance was substantially improved, beyond that of a comparable ultra high strength steel. Metallography confirmed the importance of austenite metastability in relation to fatigue crack growth rates of TRIP steels.

Further research efforts toward the goal of utilizing TRIP steels in critical applications must be predicated on the present finding concerning the paramount importance of the interrelationships between mechanical properties and austenite stability. Continued efforts are required to further elucidate these relationships. Of particular importance are studies of the effects of chemistry, prior treatment (such as warm working conditions, thermal treatment and service temperature "prior working") on starting structure, austenite metastability, and properties. Once these relationships are better understood, it is believed that TRIP steels can be tailormade to make them the optimum choice

for selected critical applications requiring a combination of strength, toughness, corrosion, and fatigue resistance not easily met by currently available ultra high strength steels."

#### CORROSION RESISTANCE

Challande[77], Padilla[78], Padilla et al[79], and Baghdasarian[80] conducted investigations to evaluate the corrosion resistance of TRIP steels in several acid and chloride ion solutions. Both general corrosion resistance and resistance to pitting were studied in TRIP steels of several different chemical compositions. Corrosion tests were conducted using the potentiodynamic polarization method developed by Edeleanu[81] and a polarization cell recommended by ASTM[82]. The scanning rate was 1.3-1.4 volts/hr. A saturated calomel electrode (SCE) was used as reference for measurement of potential.

The chemical compositions, tensile properties, and corrosion properties of several TRIP steels are summarized in Table III (adapted from [79]). The corrosion properties were determined in 2N sulfuric acid solution. The passive current densities were 8-12  $\mu\text{A per cm}^2$  corresponding to a corrosion rate of only 0.013 mm per year. Comparison with published data[83-85] indicated that the corrosion rate approached that of the AISI types 304 and 316 austenitic stainless steels. In Table IV (adapted from [80]) the anodic polarization results obtained in 2N sulfuric acid for a 13Cr-8Ni-3Mo-0.24C TRIP steel are compared with similar results obtained for annealed 304 and 316 stainless steels. It was evident that the TRIP steel and the stainless steels had approximately the same passivation potentials ( $E_p$ ) and current densities in the passive region ( $I_p$ ). The critical current density ( $I_{cr}$ ) of the TRIP steel was considerably lower than that of 304 stainless and was approximately the same as that of 316 stainless.

Although TRIP steels are designed to be used in the austenitic state, strain induced transformation of austenite may occur during use. This raises the question whether the resulting mixed austenite-martensite microstructure would have the same corrosion resistance as the original austenitic microstructure. The influence on corrosion resistance of a duplex austenite-martensite structure was investigated by Baghdasarian[80]. The corrosion properties of a 13Cr-7Ni-4Mo-0.23C TRIP steel in the austenitic condition (80% prior deformation at 500°C) were compared with the properties of the same steel with 7%, 20%, and 30% martensite (formed by cold rolling 10%, 20%, and 30% respectively at room temperature following the 80% PDA at 500°C). The results are shown in Table V (adapted from [80]). It was evident that the corrosion resistance was not appreciably altered by the presence of martensite.

In additional experiments, Baghdasarian reported that the pitting resistance (measured by the breakdown potential  $E_b$ ) in sea water of 13Cr TRIP steels was superior to that of type 316 stainless steel. Formation of 20% martensite by cold rolling resulted in enhancement of pitting resistance[80]. These results are shown in Table VI.

## HYDROGEN EMBRITTLEMENT

High strength martensitic steels are notoriously susceptible to hydrogen embrittlement which causes delayed failure at stress levels considerably lower than those causing failure in the absence of an hydrogen environment. In such steels both the time required for failure and the minimum stress for failure usually decrease as the strength is increased. Austenitic steels, on the other hand, are not embrittled in the presence of hydrogen. Metastable austenitic steels pose a unique question with regard to hydrogen embrittlement since, in the austenitic state they should be immune to embrittlement whereas embrittlement may be expected if, when deformed, they transform to martensite.

Preliminary investigations by Gold and Koppenaal[86] and McCoy et al[87] led to results which appeared to be contradicting. Gold and Koppenaal reported that TRIP steel was susceptible to hydrogen embrittlement. McCoy et al, however, noted no delayed failure in cathodically charged single edge notch TRIP steel specimens subjected to fixed loads whose maximum corresponded to 80% of the critical stress intensity. These apparently contradicting conclusions were rationalized by Zackay et al[88]. They suggested that hydrogen embrittlement of TRIP steels was a dynamic phenomenon, the most severe embrittlement being encountered at the slowest strain rates in tensile specimens, and negligible slow crack growth being observed under constant load conditions in single edge notch specimens. For embrittlement to occur, a continual new supply of martensite should be available at the tip of a crack. This continued supply is provided only under testing conditions which favor considerable strain induced transformation of austenite to martensite. At high strain rates adiabatic heating raises both the specimen temperature and the diffusivity of hydrogen. This would normally lead to more severe embrittlement. However, at

higher strain rates less time is available for diffusion and this latter factor appears to overshadow the effect of increased diffusivity. Adiabatic heating also raises austenite stability and thereby lowers its tendency to transform to martensite, and this may also be a cause of the less severe hydrogen embrittlement.

Additional studies by McCoy showed that cathodically charged single edge notch specimens did not embrittle even at low strain rates[89]. Cathodically charged tensile specimens, on the other hand, were embrittled; the loss of elongation was greater at lower strain rates.

When specimens were tested in a hydrogen atmosphere embrittlement was noted in tensile as well as single edge notch specimens. Under dynamic loading conditions in a hydrogen atmosphere single edge notch specimens exhibited embrittlement indicated by a decrease in the critical stress intensity for failure. Under fixed loading conditions they exhibited a threshold stress intensity below which slow crack growth was negligible and above which crack growth rates were proportional to  $K^{2.5}$  where K was the applied stress intensity.

#### INTERRELATIONSHIPS - STABILITY, PROCESSING, COMPOSITION, TESTING, PROPERTIES

In the foregoing discussion an attempt was made to isolate and characterize some of the structural and chemical changes that are produced by variations in the processing and testing of high strength metastable austenitic steels. These changes and their effects on stability and mechanical properties were reviewed with emphasis on variations in chemical composition, amount and temperatures of prior deformation, and testing conditions (strain rate, environment, and temperature).

The general effects of compositional, processing, and testing variables on both the stability and mechanical properties of these steels are summarized in Table VII (adapted from [36]). Vertical arrows are used to indicate whether the stability or a mechanical property is increased (arrow up) or decreased (arrow down) by a corresponding change in a particular variable. In some cases a property may change in either direction, depending on particular circumstances. Whenever the effects of a particular variable are unknown, a question mark is shown. A brief discussion of some examples taken from Table VII follows.

An increase in the alloy content of a steel will, in virtually all cases (with the possible exception of Co), increase the stability, but this is true only when the elements remain in solution in the austenite. An increase in stability usually increases yield strength because it decreases the tendency for a stress induced transformation. Elongation can either decrease or increase with an increase in stability. The elongation is high for values of  $m$  between about 0.5 and 1.0, as shown in Figure 13(a). Below 0.5 the martensite produced per unit strain is small and therefore the rate of work hardening is too low to prevent necking, and above about 1.0 the elongation decreases with decreasing stability because the large amount of martensite produced per unit strain leads to brittle failure. In general, decreasing the stability by changes in composition results in higher levels of fracture toughness [62]. For example, a steel with an  $m$  value of about two exhibited a  $K_{Ic}$  of 500,000  $\text{psi-in}^{1/2}$ . A further decrease in stability would probably have resulted in a lower fracture toughness because of the brittle fracture of the large amounts of strain induced martensite produced at the crack front.

Sauby, in unpublished work, has shown that aging thermomechanically processed "stable" austenitic steels can result in a decrease in stability and a corresponding increase in elongation with little loss in strength[90]. The effective aging temperature was at or above the PDA temperature. The influence of time at temperature of deformation (PDA), as shown in Table VII, was based on the limited results of Sauby's studies.

The relations between austenite stability and several other properties of TRIP steels are not listed in Table VII. These other properties include corrosion resistance, behavior under cyclic loading, stacking fault energy effects, impact toughness, resistance to stress corrosion, and weldability[53, 67,68,72,77-80, 92-95].

#### PRESENT STATUS OF TRIP STEEL DEVELOPMENT

Several important conclusions emerge from a review of the large number of investigations on metastable austenitic steels. First, largely by controlling a single property, namely, austenite stability, steels can be produced with a wide variety of useful combinations of engineering properties.

Another important conclusion which can be reached is that concerned with important limitations of TRIP steels. These are: their high cost which arises from expensive alloying and processing needs, and their relatively poor welding characteristics. One possible solution to the alloying problem has been suggested recently, namely, the substitution of manganese for the nickel in TRIP steels. Manganese has an added advantage, other than its lower cost, in that it promotes the formation of the hexagonal  $\epsilon$  martensite which is more resistant to hydrogen embrittlement than the bcc and bct  $\alpha'$  martensites.

Atteridge[96] has reported that by utilizing combinations of cold and warm rolling treatments in the appropriate phase fields of the Fe-Mn-C system, metastable austenitic steels can be produced with a wide range of mechanical properties. In steels containing 10-12% Mn and carbon contents from 0.2 to 1.0%, he obtained yield strengths from 75,000 to 180,000 psi and uniform elongations of 20% at a yield strength of about 120,000 psi. The inclusion of a low temperature hot rolling deformation treatment prior to warm rolling considerably reduced the amount of warm rolling that was needed to achieve the desired yield strength. Following austenitizing, the steels were cooled to a temperature corresponding to the lower end of the  $\gamma$  phase field, and were subsequently hot rolled. The steels were then warm rolled as in conventional TRIP steel processing. Based on his results Atteridge suggested that combinations of hot and warm rolling could be successfully applied to conventional TRIP steels. Although such a procedure might lead to cost savings in processing, alloying costs would not be reduced. Atteridge also suggested that with the addition of a hot rolling step, a given strength could be attained in a TRIP steel with a lower carbon content. This would be beneficial from the hydrogen embrittlement viewpoint because the lower carbon martensite forming from metastable austenite is embrittled to a lower degree than its higher carbon counterpart.

The use of manganese has also been reported in cryogenic alloys having a deformation induced transformation. In carbonless Fe-Mn alloys containing 12 to 20% Mn and with minor additions of Al and Ti, Schanfein et al[97] have reported excellent combinations of strength and Charpy V-notch impact toughness at temperatures as low as  $-196^{\circ}\text{C}$ . It has also been shown that the

stability of the austenite in these alloys can be varied considerably by variations in manganese content and by chromium additions. The addition of 0.05%C to Fe-Mn alloys was found to result in a considerable improvement in yield strength and Charpy impact toughness, with virtually no change in elongation[98].

The welding problem mentioned earlier is not unique to TRIP steels, but is common to all alloys which derive their properties from thermomechanical processing. The high temperatures encountered during welding drastically alter the nature of the austenite in TRIP steels with the result that the weld fusion zone and a large portion of the heat affected zone no longer possess the combination of high strength and ductility that existed prior to welding. It would, therefore, be desirable to resort to an alternative process which permits a postwelding treatment to restore the properties that the steel exhibited prior to welding.

Recently Koppenaal showed that thermal cycling of a kind which resulted in the formation of martensite and its subsequent reversion can produce metastable austenitic steels having high strengths[99]. In his preliminary studies with a 24Ni-4Mo-0.3C TRIP steel, Koppenaal demonstrated that a yield strength equivalent to that produced by an 80% reduction at 500°C could be attained by thermally cycling the as-austenitized steel five times between -196° and 700°C, as shown in Table VIII.

In later investigations with TRIP steels of more conventional compositions, Koppenaal reluctantly concluded that the thermal cycling process could not be conveniently used because their  $M_s$  temperatures were invariably below -196°C. In those cases where the  $M_s$  temperatures were above -196°C, he reported

that the TRIP steels did not attain properties as good as those resulting from conventional thermomechanical processing [100]. Subsequently, Adkins[101] showed that Koppenaal's thermal cycling treatment could be modified to process TRIP steels whose  $M_s$  temperatures were below  $-196^{\circ}\text{C}$ . Adkins reported high room temperature tensile strength values in TRIP steels treated by this modified process. However, stability changes occurring during processing led to yield strength and elongation values considerably lower than those resulting from conventional thermomechanical processing.

#### THE TRIP PHENOMENON IN STEELS WITH A BCC MATRIX

In recent studies Webster[102] and Antolovich et al[103] have shown that the presence of retained austenite in ferritic and martensitic steels results in a considerable improvement in fracture toughness. Other studies by Zackay et al[65], Lai et al[104,105], and Parker et al[106] have shown that the fracture toughness of as-quenched AISI 4340 steel is improved 60% by the use of a high austenitizing temperature ( $1200^{\circ}\text{C}$ ). The improvement has been attributed partly to the presence of thin films of retained austenite around martensite laths in the steel austenitized at  $1200^{\circ}\text{C}$ .

Austenite is a ductile phase which can effectively blunt propagating cracks. In addition, austenite of the right stability can transform to martensite resulting in an energy absorption ahead of a moving crack, and thereby enhance the fracture toughness. Knowledge of the beneficial influence of austenite has been used recently in improving the fracture toughness of several low and medium alloy steels. Investigations of 300-M steel and a silicon (3%) modified AISI 4340 steel have shown that isothermal transformation treatments (following austenitizing) can result in the retention of a

large amount of austenite in the bainitic matrix[107,108]. Strength-toughness combinations have been achieved approaching those of the highly alloyed maraging steels.

From the above discussion it is evident that the TRIP phenomenon can be used to enhance the toughness of high strength steels not having an austenitic matrix, and it can be considered a powerful alloy design tool for the improvement of fracture toughness at high strength levels.

#### SUMMARY

A new class of high strength steels having excellent toughness and corrosion resistance has been reported recently. These new steels derive their unique properties from metastable austenite which has been previously warm rolled to acquire high strength and which transforms, on the application of stress or strain, to martensite. The properties of these steels are primarily controlled by the stability of the austenite. Austenite stability is a function of the chemical composition of the steel, the processing variables (such as the amount and the temperature of deformation and the time at the temperature of deformation), and testing variables (such as test temperature and strain rate). With a knowledge of the variables that influence austenite stability, and of the influence of stability on properties, TRIP steels can be designed to exhibit a wide variety of properties. The high cost of alloying and processing coupled with their poor weldability has, however, limited their use. Several solutions to these problems have been suggested, including the total substitution of manganese for the nickel and the use of thermal and thermomechanical cycling. Lastly, it has been suggested that the TRIP phenomenon may be an important factor in the enhancement of the fracture toughness of high strength steels with a BCC matrix.

ACKNOWLEDGMENTS

The authors express their appreciation to Mr. M. S. Bhat for his many constructive suggestions made during the preparation of this manuscript.

This work was done under the auspices of the U. S. Atomic Energy Commission, through the Lawrence Berkeley Laboratory, Inorganic Materials Research Division, University of California, Berkeley, California 94720.

REFERENCES

1. Scheil, E., "Über die Umwandlung des Austenits in Martensite in Eisen-Nickel-legierungen unter Belastung", Z. ANORG. ALLGEM. CHEM., 207 (1932), 21-40.
2. McReynolds, A. W., "Effects of Stress and Deformation on the Martensite Transformation", J. APP. PHYS., 20 (1949), 896-907.
3. Averbach, B. L., Kulin, S. A., and Cohen, M., "The Effect of Plastic Deformation on Solid Reactions: Part II--The Effect of Applied Stress and Strain on the Martensite Reaction", in COLD WORKING OF METALS, Metals Park, Ohio: American Society for Metals (1949), 290-319.
4. Kulin, S. A., Cohen, M., and Averbach, B. L., "Effect of Applied Stress on the Martensitic Transformation", TRANS. AIME, 194 (1952), 661-68.
5. Fisher, J. C. and Turnbull, D., "Influence of Stress on Martensite Nucleation", ACTA MET., 1 (1953), 310-14.
6. Patel, J. R. and Cohen, M., "Criterion for the Action of Applied Stress on the Martensitic Transformation", Ibid., 531-38.
7. Cohen, M., Machlin, E. S., and Paranjpe, V. G., "Thermodynamics of the Martensitic Transformation", in THERMODYNAMICS IN PHYSICAL METALLURGY, Metals Park, Ohio: American Society for Metals (1950), 242-70.
8. Machlin, E. S. and Cohen, M., "The Isothermal Mode of the Martensitic Transformation", TRANS. AIME, 194 (1952), 489-500.
9. Post, C. B. and Eberly, W. S., "Stability of Austenite in Stainless Steels", TRANS. ASM, 39 (1947), 868-88.
10. Angel, T., "Formation of Martensite in Austenitic Stainless Steels: Effects of Deformation, Temperature and Composition", J. IRON STEEL INST., 177 (1954), 165-74.

11. Cina, B., "Effect of Cold Work on the  $\gamma \rightarrow \alpha$  Transformation in Some Fe-Ni-Cr Alloys", *Ibid.*, 406-22.
12. Fiedler, H. C., Averbach, B. L., and Cohen, M., "The Effect of Deformation on the Martensitic Transformation in Stainless Steels", *TRANS. ASM*, 47 (1955), 267-90.
13. Powell, G. W., Marshall, E. R., and Backofen, W. A., "Strain Hardening of Austenitic Stainless Steel", *TRANS. ASM*, 50 (1958), 478-97.
14. Shyne, J. C., Zackay, V. F., and Schmatz, D. J., "The Strength of Martensite Formed from Cold-Worked Austenite", *TRANS. ASM*, 52 (1960), 346-61.
15. Shyne, J. C., Schaller, F. W., and Zackay, V. F., "The Tensile and Yield Strength of Cr-Mn-N Steels at Low Temperatures", *Ibid.*, 848-52.
16. Guntner, C. J. and Reed, R. P., "The Effect of Experimental Variables Including the Martensitic Transformation on the Low Temperature Mechanical Properties of Austenitic Stainless Steels", *TRANS. ASM*, 55 (1962), 399-419.
17. Carlsen, K. M. and Thomas, K. C., "Effect of Composition, Heat Treatment and Cold Rolling on Mechanical Properties of Cr-Ni Stainless Steels", *Ibid.*, 462-73.
18. Breedis, J. F. and Robertson, W. D., "Martensitic Transformation and Plastic Deformation in Iron Alloy Single Crystals", *ACTA MET.*, 11 (1963), 547-59.
19. Bokros, J. C. and Parker, E. R., "The Mechanism of the Martensite Burst Transformation in Fe-Ni Single Crystals", *Ibid.*, 1291-1301.
20. Lagneborg, R., "The Martensite Transformation in 18%Cr-8%Ni Steels", *ACTA MET.*, 12 (1964), 823-43.

21. Reed, R. P. and Guntner, C. J. "Stress-Induced Martensitic Transformations in 18Cr-8Ni Steel", TRANS. MET. SOC. AIME, 230 (1964), 1713-20.
22. Bressanelli, J. P. and Moskowitz, A., "Effects of Strain Rate, Temperature and Composition on Tensile Properties of Metastable Austenitic Steels", TRANS. ASM, 59 (1966), 223-39.
23. Reed, R. P. and Breedis, J. F., "Low-Temperature Phase Transformations", in BEHAVIOR OF MATERIALS AT CRYOGENIC TEMPERATURES, ASTM Spec. Tech. Publ. 387, Philadelphia, Pennsylvania: American Society for Testing and Materials (1966), 60-132.
24. Bolling, G. F. and Richman, R. H., "The Plastic Deformation-Transformation of Paramagnetic F. C. C. Fe-Ni-C Alloys", ACTA MET., 18 (1970), 673-81.
25. Goodchild, D., Roberts, W. T., and Wilson, D. V., "Plastic Deformation and Phase Transformation in Textured Austenitic Stainless Steel", Ibid., 1137-45.
26. Tamura, I., Maki, T., Hato, H., Tomota, Y., and Okada, M., "Strength and Ductility of Austenitic Iron Alloys Accompanying Strain Induced Martensitic Transformation", in Proc. Second Int. Conf. on The Strength of Metals and Alloys, Asilomar, California, August 1970, 900-04.
27. Tamura, I., Maki, T., and Hato, H., "On the Morphology of Strain-Induced Martensite and the Transformation-Induced Plasticity in Fe-Ni and Fe-Cr-Ni Alloys", TRANS. IRON STEEL INST. OF JAPAN, 10 (1970), 163-72.
28. Richman, R. H. and Bolling, G. F., "Stress, Deformation, and Martensitic Transformation", MET. TRANS., 2 (1971), 2451-62.
29. Weiss, V., "Transformation Plasticity", Presented at Annual Pre-Congress Seminar, Detroit, Michigan, October 16-22, 1971.

30. Lecroisey, F. and Pineau, A., "Martensitic Transformations Induced by Plastic Deformation in the Fe-Ni-Cr-C System", MET TRANS. 3 (1972), 387-96.
31. Guimarães, J. R. C. and De Angelis, R. J., "Stress-Strain Relationship During Transformation Enhanced Plasticity", MET. TRANS., 4 (1973), 2379-81.
32. Maxwell, P. C., Goldberg, A., and Shyne, J. C., "Stress-Assisted and Strain-Induced Martensites in Fe-Ni-C Alloys", MET. TRANS. 5 (1974), 1305-18.
33. Maxwell, P. C., Goldberg, A., and Shyne, J. C., "Influence of Martensite Formed During Deformation on the Mechanical Behavior of Fe-Ni-C alloys", Ibid., 1319-24.
34. Zackay, V. F., Parker, E. R., Fahr, D., and Busch, R., "The Enhancement of Ductility in High Strength Steels", TRANS. ASM, 60 (1967), 252-59.
35. Gerberich, W. W., Thomas, G., Parker, E. R., and Zackay, V. F., "Metastable Austenites: Decomposition and Strength", in Proc. Second Int. Conf. on The Strength of Metals and Alloys, Asilomar, California, August 1970, 894-99.
36. Bhandarkar, D., Zackay, V. F., and Parker, E. R., "Stability and Mechanical Properties of Some Metastable Austenitic Steels", MET. TRANS., 3 (1972), 2619-31.
37. Bozorth, R. M., FERROMAGNETISM, New York: D. Van Nostrand Co. (1951).
38. Hoselitz, K., FERROMAGNETIC PROPERTIES OF METALS AND ALLOYS, Oxford, England: Clarendon Press (1952).
39. de Miramon, B., "Quantitative Investigation of Strain Induced Strengthening in Steel", M. S. Thesis, UCRL-17849, University of California, Berkeley, California, September 1967.

40. Fahr, D., "Enhancement of Ductility in High Strength Steels", Ph. D. Thesis, UCRL-19060, University of California, Berkeley, California, September 1969.
41. Fahr, D., "Stress- and Strain-Induced Formation of Martensite and its Effects on Strength and Ductility of Metastable Austenitic Stainless Steels", MET. TRANS., 2 (1971), 1883-92.
42. Stephenson, E. T. and Cohen, M., "The Effect of Prestraining and Retempering on AISI Type 4340", TRANS. ASM, 54 (1961), 72-83.
43. Zackay, V. F., Gerberich, W. W., Busch, R., and Parker, E. R., "The Strength and Toughness of Dynamically Strain Aged Alloy Steels", Proc. First Int. Conf. on Fracture, Sendai, Japan, 1965, 813-34.
44. Busch, R. A., "Strain Aging of Iron Alloys", Ph. D. Thesis, UCRL-16585, University of California, Berkeley, California, January 1966.
45. Goel, V., Busch, R., and Zackay, V. F., "Dynamic Strain Aging of a High Strength Steel", TRANS. ASME, J. BASIC ENG., 89 (1967), 871-76.
46. Kalish, D., Kulin, S. A., and Cohen, M., "Flow Strength and Fracture Toughness of 9Ni-4Co Steel as Affected by Strain Tempering and Ausforming", METALS ENG. QUART., 7 (1967), 54-61.
47. Page, E. W., "Structure and Properties of Dynamically Strain-Aged Steels", M. S. Thesis, UCRL-18244, University of California, Berkeley, California, June 1968.
48. Kalish, D. and Cohen, M., "Structural Changes and Strengthening in the Strain Tempering of Martensite", MATER. SCI. ENG., 6 (1970), 156-66.
49. Parker, E. R. and Hazlett, T. H., "Principles of Solution Hardening", in RELATION OF PROPERTIES TO MICROSTRUCTURE, Metals Park, Ohio: American Society for Metals (1954), 30-70.

50. Hall, J., Zackay, V. F., and Parker, E. R., "Structural Observations in a Metastable Austenitic Steel", TRANS. ASM, 62 (1969), 965-76.
51. Chanani, G. R., Zackay, V. F., and Parker, E. R., "Tensile Properties of 0.05 to 0.20 Pct C TRIP Steels", MET. TRANS., 2 (1971), 133-39.
52. Austin, J. B. and Rickett, R. L., "Kinetics of Decomposition of Austenite at Constant Temperatures", TRANS. AIME, 135 (1939), 396-415.
53. Weiss, V., Schroder, K., Sanford, W., Chandan, H., Kunio, T., Lal, D., and Sengupta, M., "The Relationships Between the Transformation Characteristics and the Fracture and Fatigue Properties of TRIP Steel", Syracuse University, Department of Chemical Engineering and Materials Science, Syracuse, New York, Army Materials and Mechanics Research Center, Watertown, Massachusetts, Tech. Rep. AMMRC CTR 73-50, December 1973.
54. Schwartzberg, F. R., Osgood, S. H., Keys, R. D., and Kiefer, T. I., CRYOGENIC MATERIALS DATA HANDBOOK, Tech. Documentary Rep. ML-TDR-64-280, Denver, Colorado: Martin Company (1964).
55. Kula, E. B. and DeSisto, T. S., "Plastic Behavior of Metals at Cryogenic Temperatures", in BEHAVIOR OF MATERIALS AT CRYOGENIC TEMPERATURES, ASTM Spec. Tech. Publ. 387, Philadelphia, Pennsylvania: American Society for Testing and Materials (1966), 3-31.
56. Laporte, C. P., "Effect of a Strain Induced Transformation on the Toughness of High Strength Materials", M. S. Thesis, UCRL-17810, University of California, Berkeley, California, September 1967.
57. Gerberich, W. W., Hemmings, P. L., Merz, M. D., and Zackay, V. F., "Preliminary Toughness Results on TRIP Steel", TRANS. ASM, 61 (1968), 843-47.

58. Antolovich, S. D., "Fracture Toughness and Strain Induced Phase Transformations", TRANS. MET. SOC. AIME, 242 (1968), 2371-73.
59. Gerberich, W. W., Hemmings, P. L., Zackay, V. F., and Parker, E. R., "Interactions Between Crack Growth and Strain Induced Transformations", in FRACTURE 1969, ed. by P. L. Pratt, London: Chapman and Hall Ltd. (1969), 288-305.
60. Gerberich, W. W. and Birat, J. P., "A Metastable Austenite with Plane Stress Fracture Toughness near  $500,000 \text{ psi-in}^{1/2}$ ", INT. J. FRACT. MECH., 7 (1971), 108-10.
61. Antolovich, S. D. and Singh, B., "On the Toughness Increment Associated with the Austenite to Martensite Phase Transformation in TRIP Steels", MET. TRANS., 2 (1971), 2135-41.
62. Gerberich, W. W., Hemmings, P. L., and Zackay, V. F., "Fracture and Fractography of Metastable Austenites", MET. TRANS., 2 (1971), 2243-53.
63. Antolovich, S. D. and Fahr, D., "An Experimental Investigation of the Fracture Characteristics of TRIP Alloys", ENG. FRACT. MECH., 4 (1972), 133-44.
64. Parker, E. R. and Zackay, V. F., "Enhancement of Fracture Toughness in High Strength Steel by Microstructural Control", ENG. FRACT. MECH., 5 (1973), 147-65.
65. Zackay, V. F., Parker, E. R., and Wood, W. E., "Influence of Some Microstructural Features on the Fracture Toughness of High Strength Steels", MICROSTRUCTURE AND DESIGN OF ALLOYS, London, England: Institute of Metals (1973), 175-79.

66. "Standard Method of Test for Plane Strain Fracture Toughness of Metallic Materials", E 399-72 in ANNUAL BOOK OF ASTM STANDARDS, Part 31, Philadelphia, Pennsylvania: American Society for Testing and Materials (1973), 960-79.
67. Chanani, G. R., "Fracture Characteristics of Metastable Austenitic Steels Under Cyclic Loading", D. Eng. Thesis, UCRL-19620, University of California, Berkeley, California, July 1970.
68. Chanani, G. R. and Antolovich, S. D., "Low Cycle Fatigue of a High Strength Metastable Austenitic Steel", MET. TRANS., 5 (1974), 217-29.
69. Coffin, L. F., Jr. and Tavernelli, J. F., "The Cyclic Straining and Fatigue of Metals", TRANS. MET. SOC. AIME, 215 (1959), 794-807.
70. Coffin, L. F., Jr., "Low Cycle Fatigue: A Review", APP. MATER. RES., 1, No. 3 (1962), 129-41.
71. Manson, S. S., "Fatigue: A Complex Subject--Some Simple Approximations", EXP. MECH., 5 (1965), 193-226.
72. Chanani, G. R., Antolovich, S. D., and Gerberich, W. W., "Fatigue Crack Propagation in TRIP Steels", MET. TRANS., 3 (1972), 2661-72.
73. Paris, P. C. and Erdogan, F., "A Critical Analysis of Crack Propagation Laws", TRANS. ASME, J. BASIC ENG., 85 D (1963), 528-34.
74. Wei, R. P., Talda, P. M., and Li, Che-Yu, "Fatigue Crack Propagation in Some Ultrahigh-Strength Steels", in FATIGUE CRACK PROPAGATION, ASTM Spec. Tech. Publ. 415, Philadelphia, Pennsylvania: American Society for Testing and Materials (1967), 460-85.
75. Donaldson, D. R. and Anderson, W. E., "Crack Propagation Behavior of Some Airframe Materials", in Proc. Crack Propagation Symp., Cranefield, England, Vol. 2 (1961), 375-442.

76. Carman, C. M. and Katlin, J. M., "Low Cycle Fatigue Crack Propagation Characteristics of High Strength Steels", 66-MET-3, TRANS. ASME, J. BASIC ENG., 88 D (1966), 792-800.
77. Challande, J. F., "Corrosion Resistance of Metastable Austenitic Steels", M. S. Thesis, UCRL-18475, University of California, Berkeley, California, September 1968.
78. Padilla, F. J., "Optimization of Corrosion Resistance in Metastable Austenitic Steel", M. S. Thesis, UCRL-19065, University of California, Berkeley, California, September 1969.
79. Padilla, F. J., Challande, J. F., and Ravitz, S. F., "Effect of Composition on the Corrosion Resistance of Some Ultra-High Strength Metastable Austenitic Steels", UCRL-19657, Lawrence Berkeley Laboratory, Berkeley, California, June 1970.
80. Baghdasarian, A. J., "Corrosion Resistance of TRIP Steels", M. S. Thesis, LBL-806, University of California, Berkeley, California, May 1972.
81. Edeleanu, C., "Method for the Study of Corrosion Phenomena", NATURE, 173 (1954), 739.
82. "Standard Reference Method for Making Potentiostatic and Potentiodynamic Anodic Polarization Measurements", G5-69 in ANNUAL BOOK OF ASTM STANDARDS, Part 24, Philadelphia, Pennsylvania: American Society for Testing and Materials (1970).
83. Fontana, M. and Greene, N., CORROSION ENGINEERING, New York: McGraw-Hill Book Co., Inc. (1967).
84. France, W. D., Jr. and Lietz, R. W., "Improved Data Recording for Automatic Potentiodynamic Polarization Measurements", CORROSION, 24 (1968), 298-300.

85. Wilde, B. E. and Greene, N. D., Jr., "The Variable Corrosion Resistance of 18Cr-8Ni Stainless Steels: Behavior of Commercial Alloys", CORROSION, 25 (1969), 300-06.
86. Gold, E. and Koppenaal, T. J., "Anomalous Ductility of TRIP Steel", TRANS. ASM, 62 (1969), 607-10.
87. McCoy, R. A., Gerberich, W. W., and Zackay, V. F., "On the Resistance of TRIP Steel to Hydrogen Embrittlement", MET. TRANS., 1 (1970), 2031-34.
88. Zackay, V. F., Gerberich, W. W., and Ravitz, S. F., "Mechanical Properties and Corrosion Resistance of TRIP Steels", Presented at the Western Tech. Conf., Los Angeles, California, March 1971. Also, UCRL-20523, Lawrence Berkeley Laboratory, Berkeley, California, February 1971.
89. McCoy, R. A., "The Resistance of TRIP Steels to Hydrogen Embrittlement", D. Eng. Thesis, LBL-135, University of California, Berkeley, California, September 1971.
90. Sauby, M. E., "The Investigation of High Strength in High Carbon Stainless Steels", M. S. Thesis, UCRL-19678, University of California, Berkeley, California, September 1970.
91. Goldberg, A. and Hoge, K. G., "Effect of Strain Rate on Tension and Compression Stress-Strain Behavior in a TRIP Alloy", MATER. SCI. ENG., 13 (1974), 211-22.
92. Dokko, C., "TRIP Phenomena in Impact Tests", M. S. Thesis, UCRL-19068, University of California, Berkeley, California, September 1969.
93. Dunning, J. S., "The Effect of Stacking Fault Energy on the Strain Induced Martensite Transformation and Tensile Characteristics in Iron Based Alloys", Ph. D. Thesis, UCRL-19052, University of California, Berkeley, California, December 1969.

94. Ambekar, S. M., "Joining TRIP Steels", D. Eng. Thesis, UCRL-19129, University of California, Berkeley, California, February 1970.
95. Birat, J. P., "Stress Corrosion Cracking of a TRIP Steel", M. S. Thesis, UCRL-20300, University of California, Berkeley, California, September 1970.
96. Atteridge, D. G., "An Investigation of the Structure and Properties of Iron-Manganese-Carbon Alloys", D. Eng. Thesis, University of California, Berkeley, California (In preparation).
97. Schanfein, M. J., Yokota, M. J., Zackay, V. F., Parker, E. R., and Morris, J. W., Jr., "The Cryogenic Properties of Fe-Mn and Fe-Mn-Cr Alloys, Presented at the ASTM Symp. on Properties of Materials for Liquid Natural Gas Tankage, Boston, Massachusetts, May 21-22, 1974. Also, LBL-2764, Lawrence Berkeley Laboratory, Berkeley, California, May 1974.
98. Schanfein, M. J., "The Cryogenic Properties of Fe-Mn and Fe-Mn-Cr Alloys", M. S. Thesis, LBL-2749, University of California, Berkeley, California, August 1974.
99. Koppenaar, T. J., "A Thermal Processing Technique for TRIP Steels", MET. TRANS., 3 (1972), 1549-54.
100. Koppenaar, T. J., "Research in Development of Improved TRIP Steels", Philco-Ford Corporation, Aeronutronic Division, Newport Beach, California, Army Materials and Mechanics Research Center, Watertown, Massachusetts, Contract No. DAAG46-72-C-0047, Final Rep. AMMRC CTR 73-4, January 1973.
101. Adkins, H. E., Jr., "Structure and Properties of TRIP Steels Processed by Deformation and Thermal Cycling", M. S. Thesis, LBL-1491, University of California, Berkeley, California, April 1973.

102. Webster, D., "Development of a High Strength Stainless Steel with Improved Toughness and Ductility", MET. TRANS., 2 (1971), 2097-104.
103. Antolovich, S. D., Saxena, A., and Chanani, G. R., "Increased Fracture Toughness in a 300 Grade Maraging Steel as a Result of Thermal Cycling", MET. TRANS., 5 (1974), 623-32.
104. Lai, G. Y., Wood, W. E., Clark, R. A., Zackay, V. F., and Parker, E. R., "The Effect of Austenitizing Temperature on the Microstructure and Mechanical Properties of As-Quenched 4340 Steel", Ibid., 1663-70.
105. Lai, G. Y., Wood, W. E., Zackay, V. F. and Parker, E. R., "Influence of Microstructural Features on Fracture Toughness of an Ultra-High Strength Steel, LBL-2236, Lawrence Berkeley Laboratory, Berkeley, California (In preparation).
106. Parker, E. R., Zackay, V. F., Lai, G. Y., and Horn, R. M., "Untempered Ultra-High Strength Steels of High Fracture Toughness", LBL-2715, Lawrence Berkeley Laboratory, Berkeley, California, Army Materials and Mechanics Research Center, Contract No. DAAG46-73-C-0120, Final Rep. AMMRC CTR 74-33, April 1974.
107. Babu, B. N. P., "An Investigation of Bainite Transformation in Medium Carbon Low Alloy Steels", D. Eng. Thesis, LBL-2772, University of California, Berkeley, California, August 1974.
108. Lai, G. Y., Zackay, V. F., and Parker, E. R. "Enhancement of Fracture Toughness in a Low Alloy Steel by Retained Austenite as a Result of Upper Bainite Reaction", Lawrence Berkeley Laboratory, Berkeley, California (In preparation).

TABLE I  
Chemical Compositions of Some TRIP Alloys

Designation	Compositions, Wt %			
	C	Ni	Cr	Mn
34N	< 0.010	33.7	-	-
38N	< 0.010	37.8	-	-
CN28	0.294	28.0	-	0.5
CN8Cr	0.325	8.0	9.0	2.0
CN12Cr	0.290	12.0	9.0	2.0
CN16Cr	0.292	16.0	9.0	2.0
CN21Cr	0.287	21.4	9.0	2.0

TABLE II  
Estimated  $M_s$  and  $M_d$  Temperatures of Some TRIP Alloys

Designation	Thermomechanical Process	Estimation of $M_s$		Estimation of $M_d$	
		$M_s$ , °C	Technique Used	$M_d$ , °C	Technique Used
34N	70% PDA at temperatures between 22°C and 450°C	-85	Resistivity	10-22	Tension test*
38N	Same as above	<-196	Resistivity	About -150°C	Tension test
CN28	Same as above	-68	Resistivity	About 25°C	Tension test
CN8Cr	For estimation of $M_s$ only: 70% PDA at temperatures between 22°C and 450°C	<-196	Magnetic measurements	150°C	70% deformation by rolling**
CN12Cr	Same as for 34N	<-196	Magnetic measurements	22°C	Tension Test
CN16Cr	Same as for CN8Cr	<-196	Magnetic measurements	About -120°C	70% deformation by rolling
CN21Cr	Same as for 34N	<-196	Magnetic measurements	About -196°C	Tension test

\*The alloy after thermomechanical processing was tested in tension at various temperatures and the  $M_d$  was estimated as the temperature above which no deformation induced martensite formed.

\*\*The alloy was examined after 70% PDA at several temperatures and the  $M_d$  was estimated as that above which no deformation induced martensite formed.

TABLE III  
 Chemical Composition, and Tensile and Corrosion Properties  
 of 13Cr-0.25C TRIP Steels as a Function of Ni, Mo, and Mn Contents

Alloy	Ni, Mo, Mn Contents, wt %			Passive Current Density ( $I_p$ ) $\mu$ amp/cm <sup>2</sup>	Critical Current Density ( $I_{cr}$ ) $\mu$ amp/cm <sup>2</sup>	Primary Passive Potential† ( $E_p$ ) Volts vs SCE	Strength, 10 <sup>3</sup> psi		Elong. %	Reduction in Area, %
	Ni	Mo	Mn				Yield	Tensile		
A	8	-	-	12	1,000	-0.34	164	253	28	32
B	11	-	-	11	750	-0.32	187	187	8	51
C	10	1	-	12	100	-0.31	194	194	11	51
D	9	2	-	12	35	-0.27	200	209	46	44
E	8	1	-	12	75	-0.32	190	264	27	35
F	8	3	-	8	15	-0.25	187	231	38	38
G	7	4	-	10	15	-0.24	185	249	34	42
H	6	3	2	9	30	-0.28	185	231	40	33
I	6	3	4	10	35	-0.38	186	188	46	42

All steels were austenitized at 1200°C, quenched in ice brine, reduced 80% in thickness at 450°C (PDA).

†The corrosion potential was consistently 0.04 to 0.05v more negative.

TABLE IV  
 Anodic Polarization Results for a 13Cr-8Ni-3Mo-0.24C  
 TRIP Steel and Stainless Steels 304 and 316

Alloy	Source	$E_p$ Volts vs SCE	$I_{cr}$ $\mu$ amp/cm <sup>2</sup>	$I_p$ $\mu$ amp/cm <sup>2</sup>
304 Stainless	Baghdasarian [80]	-.24	72	8
	Padilla [78]	-.22	84	4
	France & Lietz [84]	-.30	35	7
316 Stainless	Baghdasarian [80]	-.20	12	4
	Fontana & Greene [83]	-.18	15	2
	Wilde & Greene [85]	-.22	9	-
13Cr-8Ni- 3Mo-0.24C TRIP Steel	Baghdasarian [80]	-.24	17	7
	Padilla [78]	-.25	15	8

TABLE V  
Corrosion Properties of a 13Cr-7Ni-4Mo-0.23C  
TRIP Steel as a Function of Martensite Content\*

% Martensite	$E_o$ Volts vs SCE	$E_p$ Volts vs SCE	$I_{cr}$ $\mu$ amp/cm <sup>2</sup>	$I_p$ $\mu$ amp/cm <sup>2</sup>
0	-.23	-.22	6.1	3.1
7	-.25	-.20	6.2	3.1
20	-.28	-.24	8.6	4.3
30	-.30	-.26	11.4	4.3

\*Strain induced martensite was formed by cold rolling at room temperature.

TABLE VI  
Breakdown Potentials ( $E_b$ ) in Sea Water for  
Several 13Cr TRIP Steels and Type 316 Stainless Steel

No.	Steel	$E_b$ (Volts)
1	316 Stainless	+ 0.29
2	13Cr-8Ni-3Mo-0.24C TRIP Steel	+ 0.42
3	13Cr-7Ni-4Mo-0.23C TRIP Steel	+ 0.65
4	TRIP Steel 3 Cold-rolled at 22°C to form 20% Martensite	+ 0.84

TABLE VII  
 Probable Relationships Between Stability, as Affected by Several Compositional,  
 Processing and Testing Variables, and Selected Mechanical Properties

Variable	Stability	Mechanical Property					
		Yield Strength	Lüders Strain	Elongation	Work Hardening Rate	Fracture Toughness	Resistance to Hydrogen Embrittlement
<b>COMPOSITION (increasing)</b>							
Substitutional solutes (exception of Co)	↑ [35,36,40]	↑ [36,40]	↑ [35,36,40]	↑↑ [35,36,40]	↓ [36,40]	↓ [62]	↑ [87-89]
Interstitial solutes (C and N)	↑ [35,40,41,51]	↑ [40,41,51]	↑ [35,40,41,51]	↑↑ [35,40,41,51]	↓ [40,41,51]	↓ [62]	↑↑ [87-89]
<b>PROCESSING (All variables increasing)</b>							
Amount of deformation (PDA)	↑↑ [35]	↑↑ [35,40,41,50]	↑↑ [35,40,41]	↑↑ [35,40,41,50]	↑↑ [40,41,50]	↑ [62]	↓ [87-89]
Temperature of deformation (PDA)	↑↑ [36]	↑↑ [36]	↑↑ [36]	↑↑ [36]	↑↑ [36]	↑↑ [62]	↑↑ [87-89]
Time at temperature of deformation (PDA)	↓ [90]	↑ [90]	↓ [90]	↑↑ [90]	↑ [90]	?	↓ [87-89]
<b>TESTING</b>							
Test temperature (decreasing)	↓ [35,36,40,41,51]	↑↑ [35,36,40,41,51]	↑↑ [35,36,40,41,51]	↑↑ [35,36,40,41,51]	↑↑ [35,36,40,41,51]	↑↑ [57,59,62]	↑↑ [86-89]
Strain rate (increasing)	↑ [22,91]	↑↑ [22,91]	↑↑ [22,91]	↑↑ [22,91]	↑↑ [22,91]	↑↑ [57,59,62]	↑↑ [86-89]

Note: [ ] refers to relevant paper in the bibliography.

TABLE VIII  
Room Temperature Mechanical Properties of  
a Fe-24Ni-4Mo-0.3C TRIP Steel

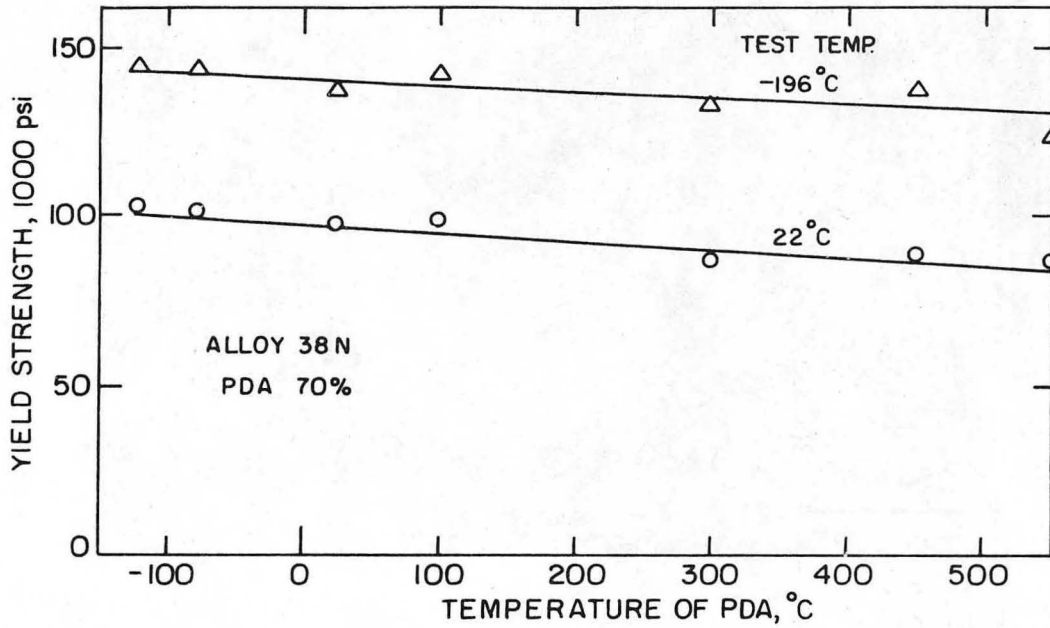
Type of Processing	Yield Strength, 10 <sup>3</sup> psi	Ultimate Tensile Strength, 10 <sup>3</sup> psi	Elongation, %
Thermomechanical (80% reduction at 500°C)	164	176	41
Thermal (5 cycles between -196°C and 700°C)	162	193	30

FIGURE CAPTIONS

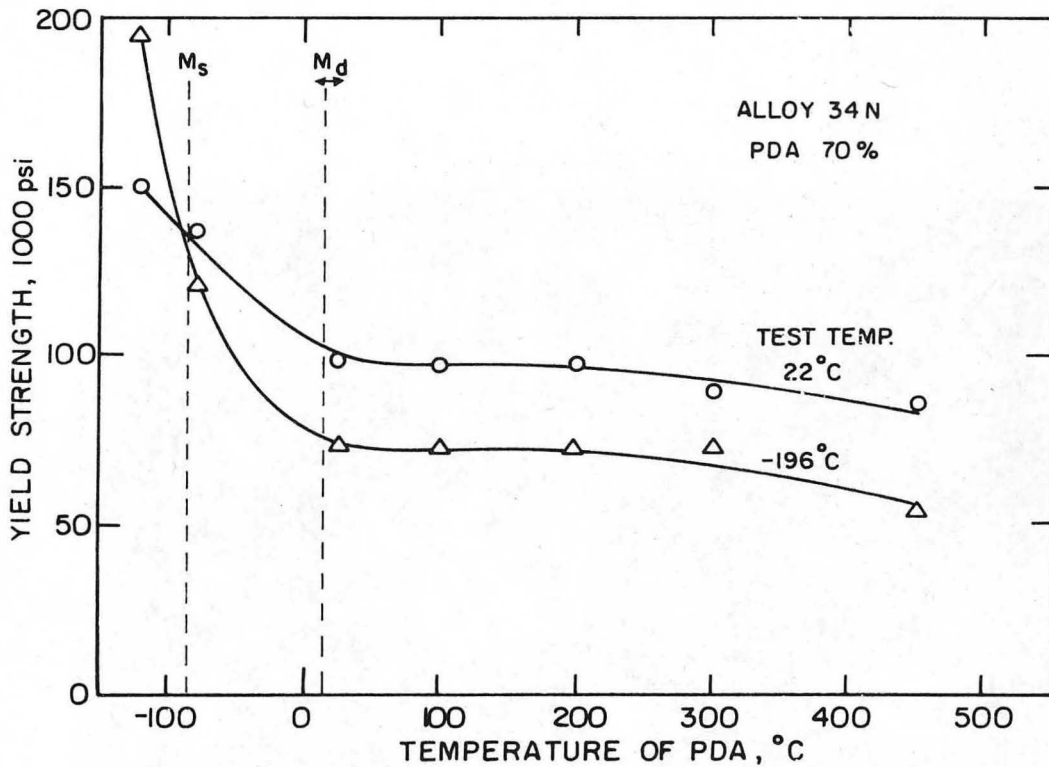
1. The effect of PDA temperature on the yield strengths of (a) alloy 38N, deformed 70% at the indicated temperatures (stable at all processing temperatures), and (b) alloy 34N, deformed 70% at the indicated temperatures (unstable below the  $M_d$ ) [36].
2. Photomicrographs of specimens of alloy 34N, before testing: (a) rolled at a PDA temperature of  $-120^{\circ}\text{C}$ , showing martensite produced during rolling; (b) rolled above the  $M_d$  and cooled to  $-196^{\circ}\text{C}$ , showing the athermal martensite produced during cooling to the test temperature [36].
3. Typical engineering stress-strain curves for alloy 34N, at test temperatures of  $22^{\circ}$  and  $-196^{\circ}\text{C}$ , deformed 70% at a PDA temperature of  $450^{\circ}\text{C}$  [36].
4. The effect of PDA temperature on the yield strength of alloy 34N, deformed 70% and tested at  $22^{\circ}$  and  $-78^{\circ}\text{C}$  [36].
5. The engineering stress-strain curves of alloy 34N, deformed 70% at PDA temperatures of (a)  $25^{\circ}$ , (b)  $200^{\circ}$ , and (c)  $450^{\circ}\text{C}$  [36].
6. The effect of PDA temperature on the yield strength of steel CN28 at test temperatures of  $22^{\circ}$  and  $-78^{\circ}\text{C}$ . The steel was deformed 70% at the indicated temperatures [36].
7. The effect of PDA temperature on the room temperature yield strengths of steels CN8Cr, CN12Cr, and CN21Cr, deformed 70% at the indicated temperatures [36].
8. The effect of PDA temperature on the  $-78^{\circ}\text{C}$  yield strengths of the steels shown in Figure 7 [36].

9. Plots of room temperature yield strength vs amount of prior deformation (PDA), at 450°C, for 9Cr-8Ni-2Mn steels with carbon contents as indicated (adapted from [41]).
10. Effect of the amount of prior deformation (PDA), at 450°C, on the room temperature engineering stress-strain curves of a 9Cr-8Ni-3Mn-0.4C TRIP steel (adapted from [41]).
11. Effect of the amount of prior deformation (PDA), at 450°C, on the room temperature engineering stress-strain curves of a 9Cr-8Ni-2Mn-0.2C TRIP steel (adapted from [41]).
12. The relation between strain and the volume fraction of martensite that is produced in steel CN8Cr, deformed 70% at 450°C, for test temperatures of (a) 22°, (b) -78°, (c) -196°, and (d) -78° and -196°C (after correcting for the fact that the volume fraction of stress induced martensite formed at -78°C was 0.15 greater than that formed at -196°C) [36]. The curves representing the relationship of  $V_{\alpha}$  and  $\epsilon$  suggested by Angel [10] and Gerberich et al [35] are also shown.
13. The correlation between the stability coefficient,  $m$ , and (a) the elongation to fracture, (b) the Lüders strain for a large group of TRIP alloys of widely varying compositions and processing histories (adapted from [35]).
14. The engineering stress-strain curves of steel CN8Cr, deformed 70% at 450°C (PDA), at test temperatures indicated. The values of the stability coefficient,  $m$ , determined from the data of Fig. 12 are also shown [36].
15. The engineering stress-strain curves for three steels of differing nickel content (8, 12, and 16%), deformed 70% at 450°C (PDA) and tested at -78°C. The values of the stability coefficient,  $m$ , are shown [36].

16. The room temperature engineering stress-strain curves of steel CN8Cr, deformed 70% at PDA temperatures of 200° and 450°C. The values of the stability coefficient,  $m$ , are shown (adapted from [36]).
17. Influence of austenite stability ( $m$  value) on the plane stress fracture toughness of high strength metastable austenites (adapted from [62]).
18. Effect of carbon content on cleavage of martensite and, hence, on apparent  $K_{Ic}$  at -196°C[62].
19. Effect of thickness on the critical stress intensity factors at room temperature for TRIP steel and two commercial steels (adapted from [62]).
20. Plots of fracture toughness vs yield strength. Bands for TRIP steels ( $K_c$ ) and commercial steels ( $K_{Ic}$ )[65].



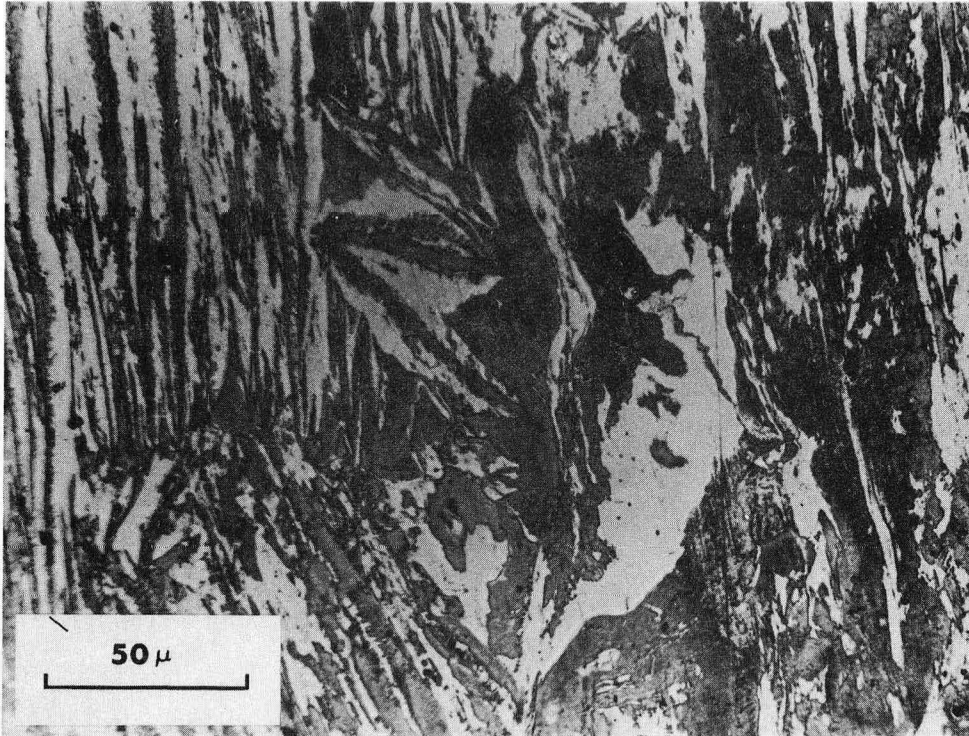
(a)



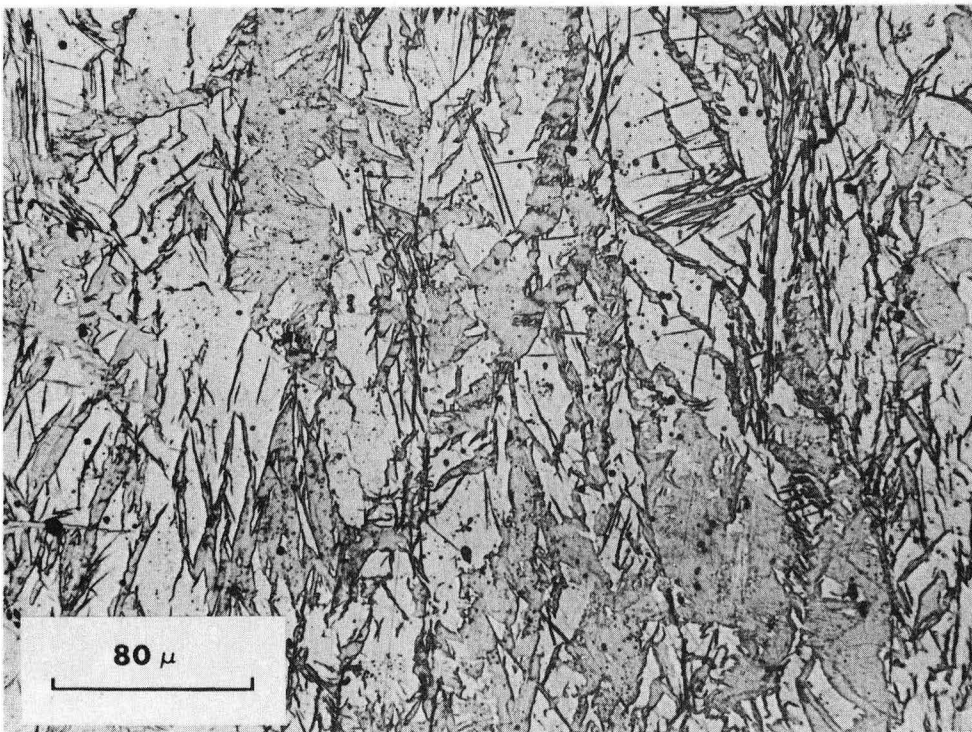
(b)

XBL 7110-7490

Fig. 1



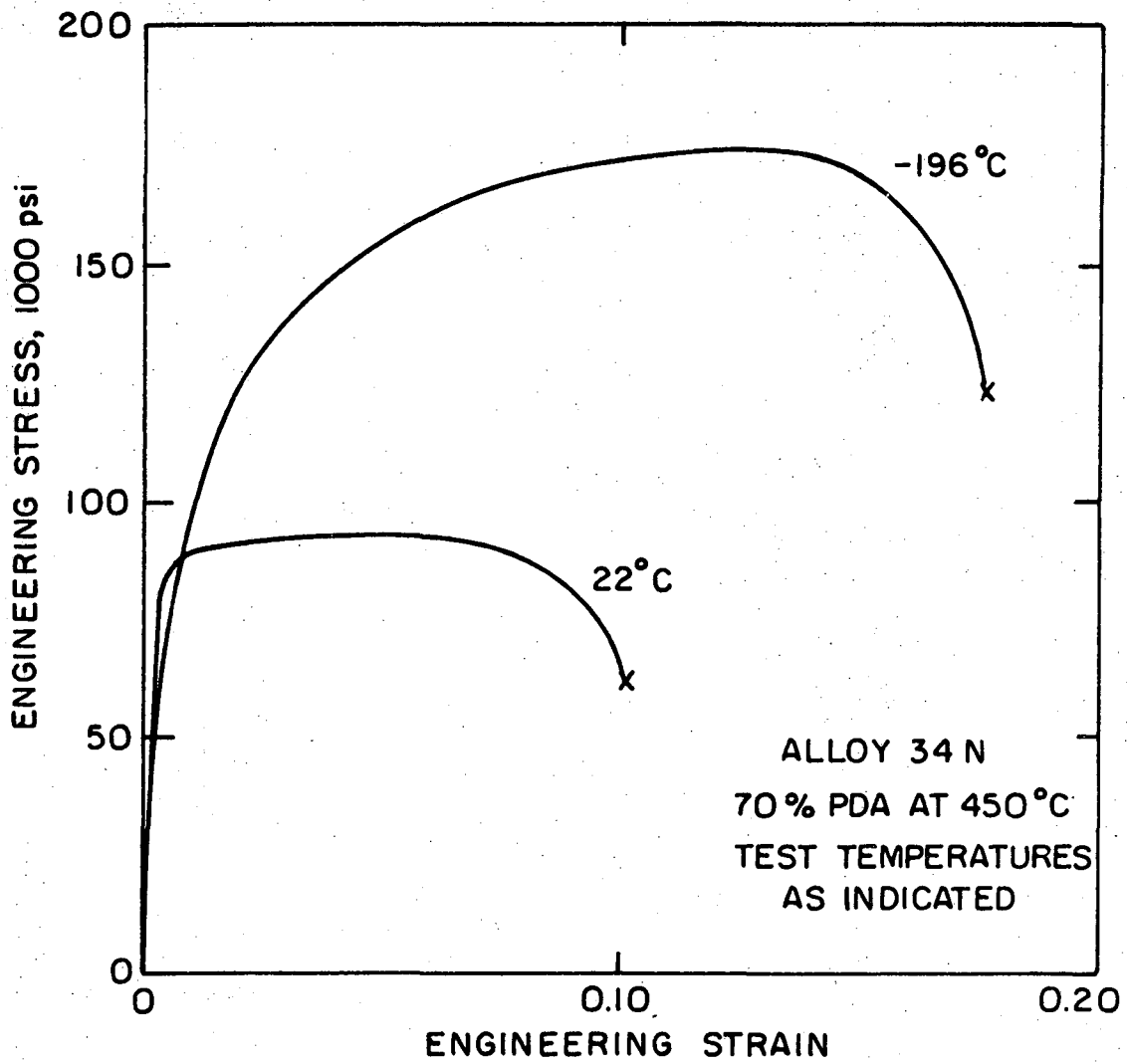
(a)



(b)

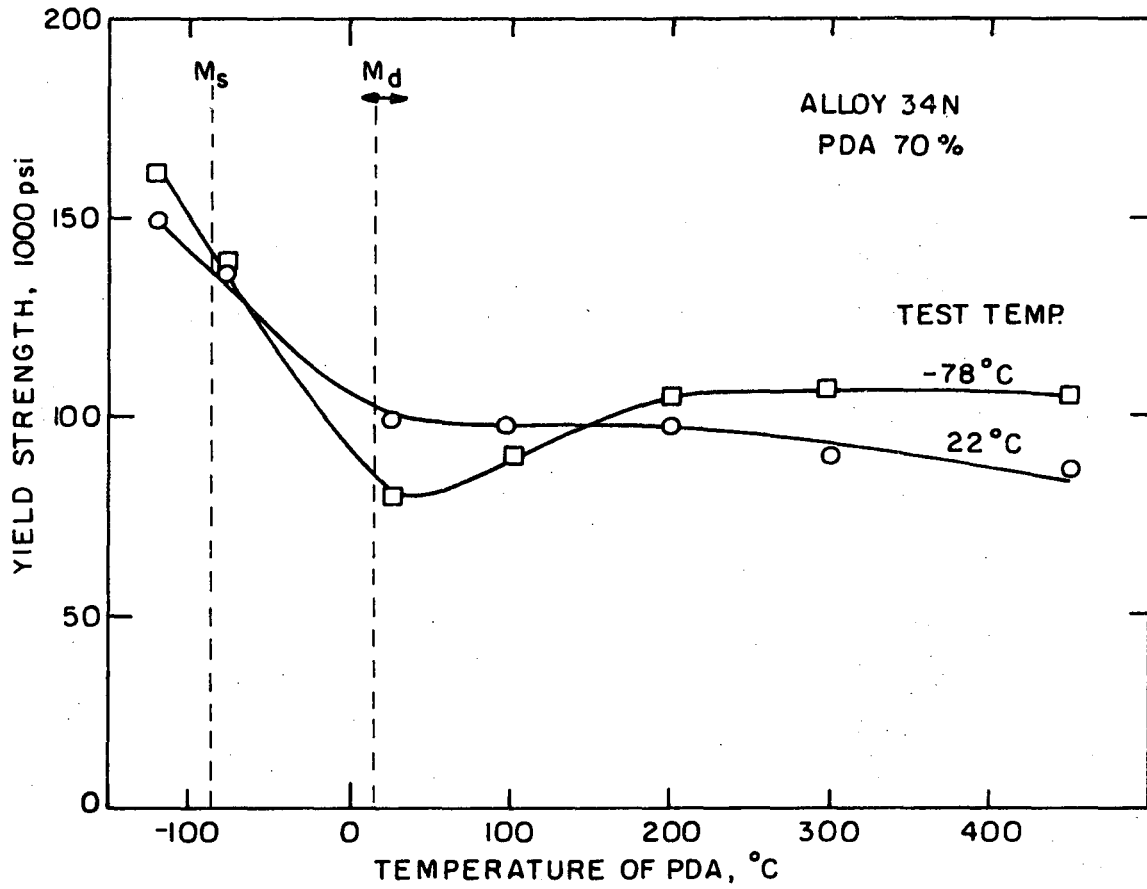
XBB 7111-5605

Fig. 2



XBL 7110-7491

Fig. 3



XBL 7110-7492

Fig. 4

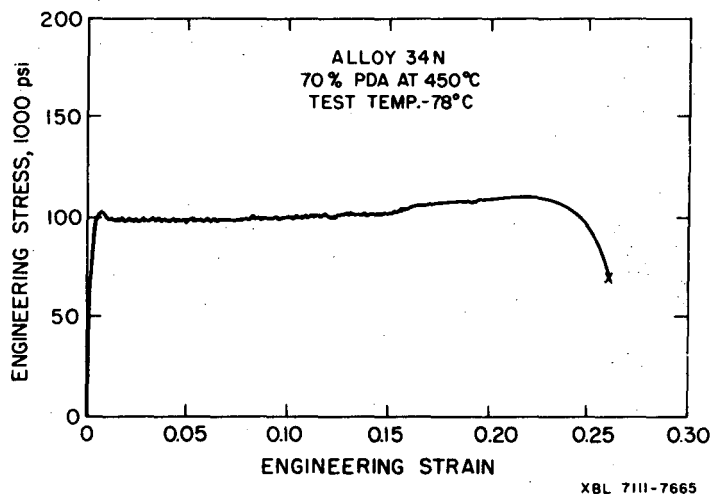
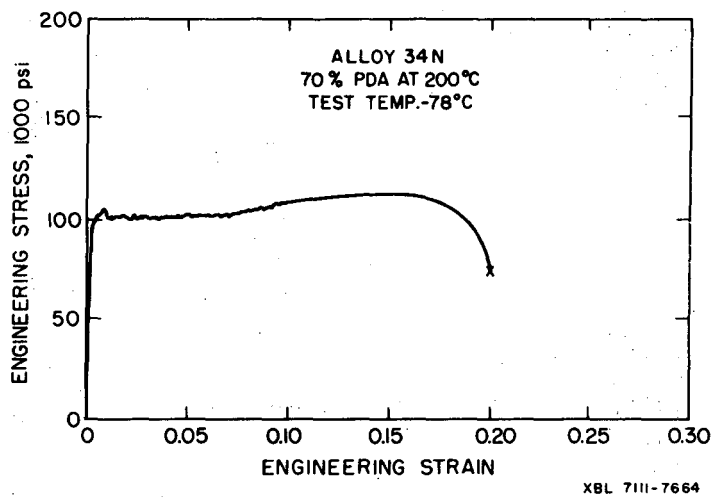
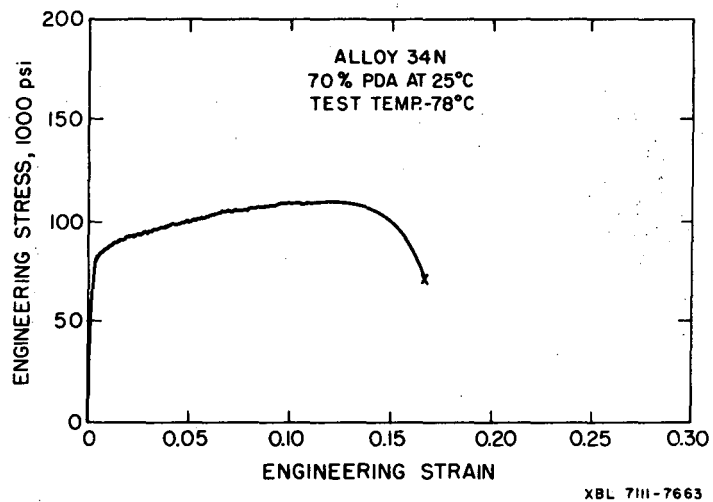
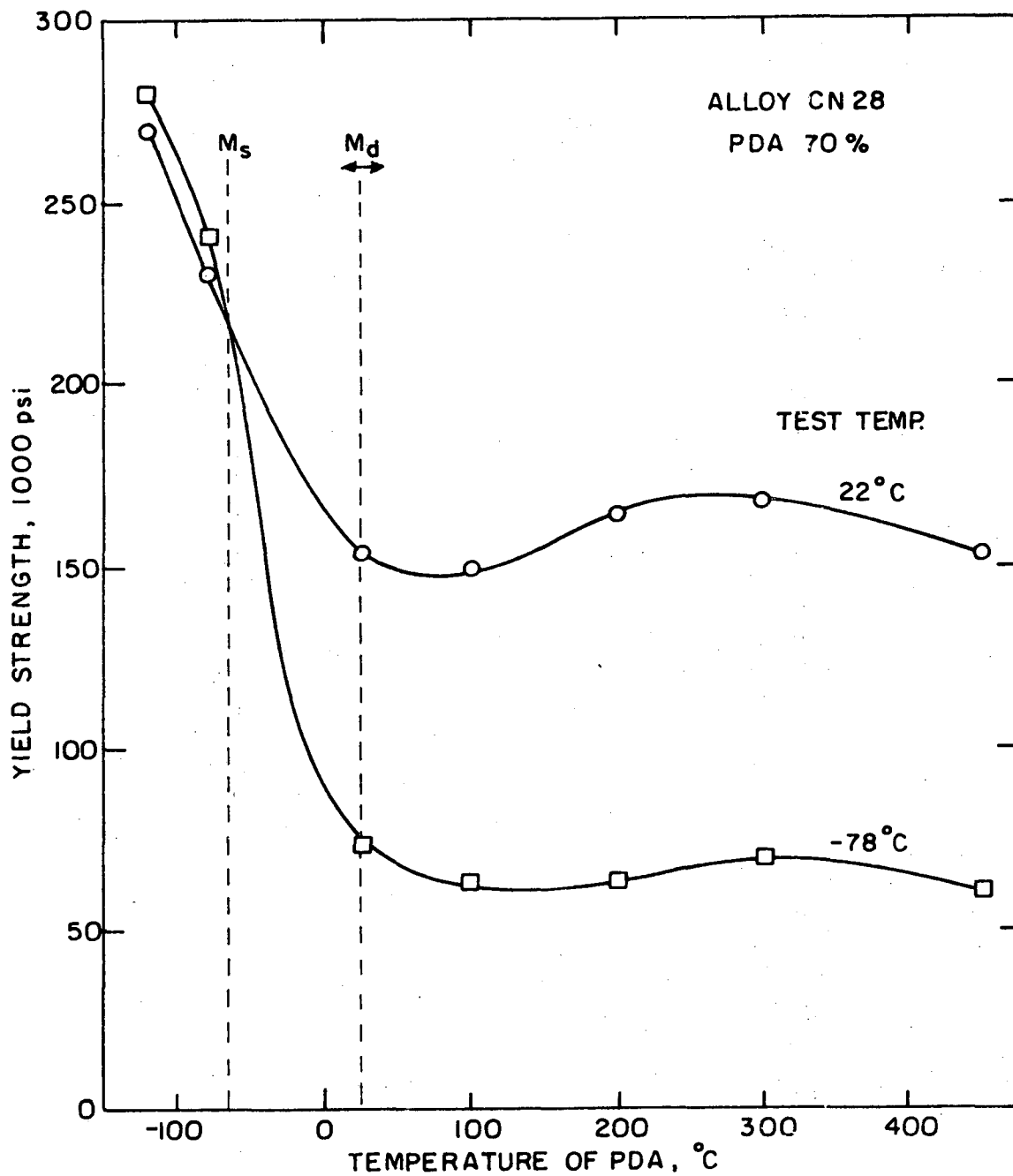
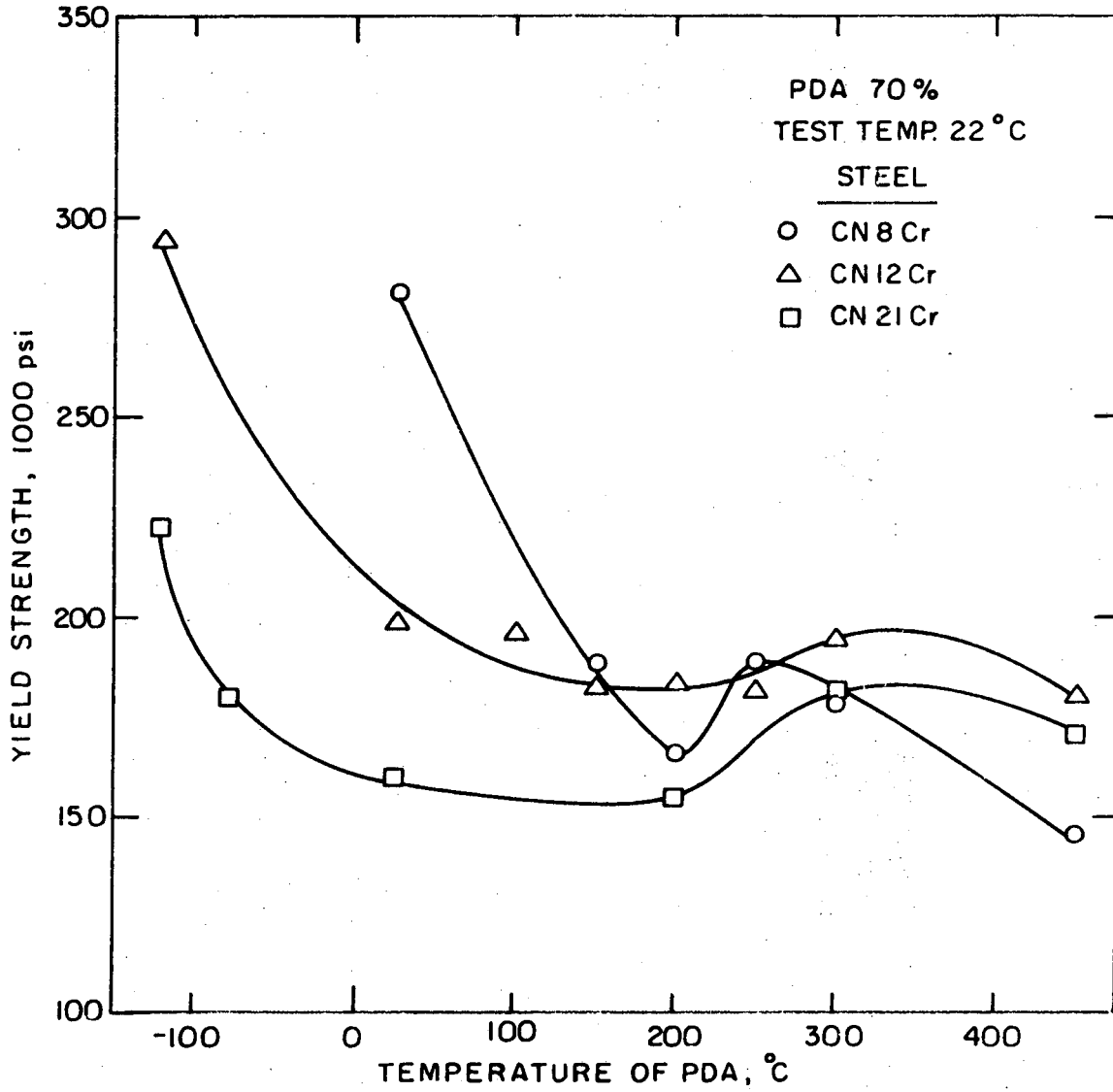


Fig. 5



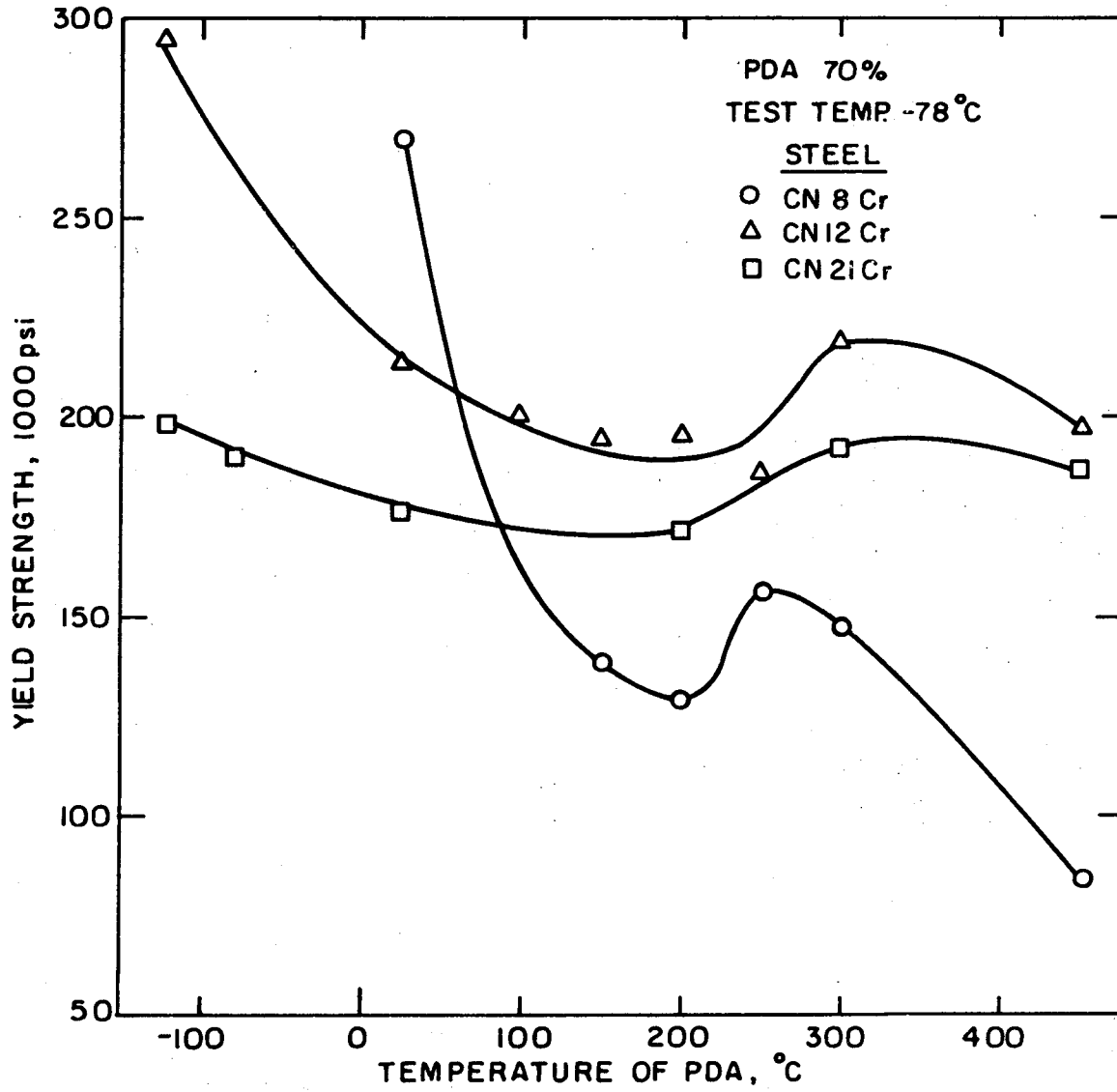
XBL 7110 7496

Fig. 6



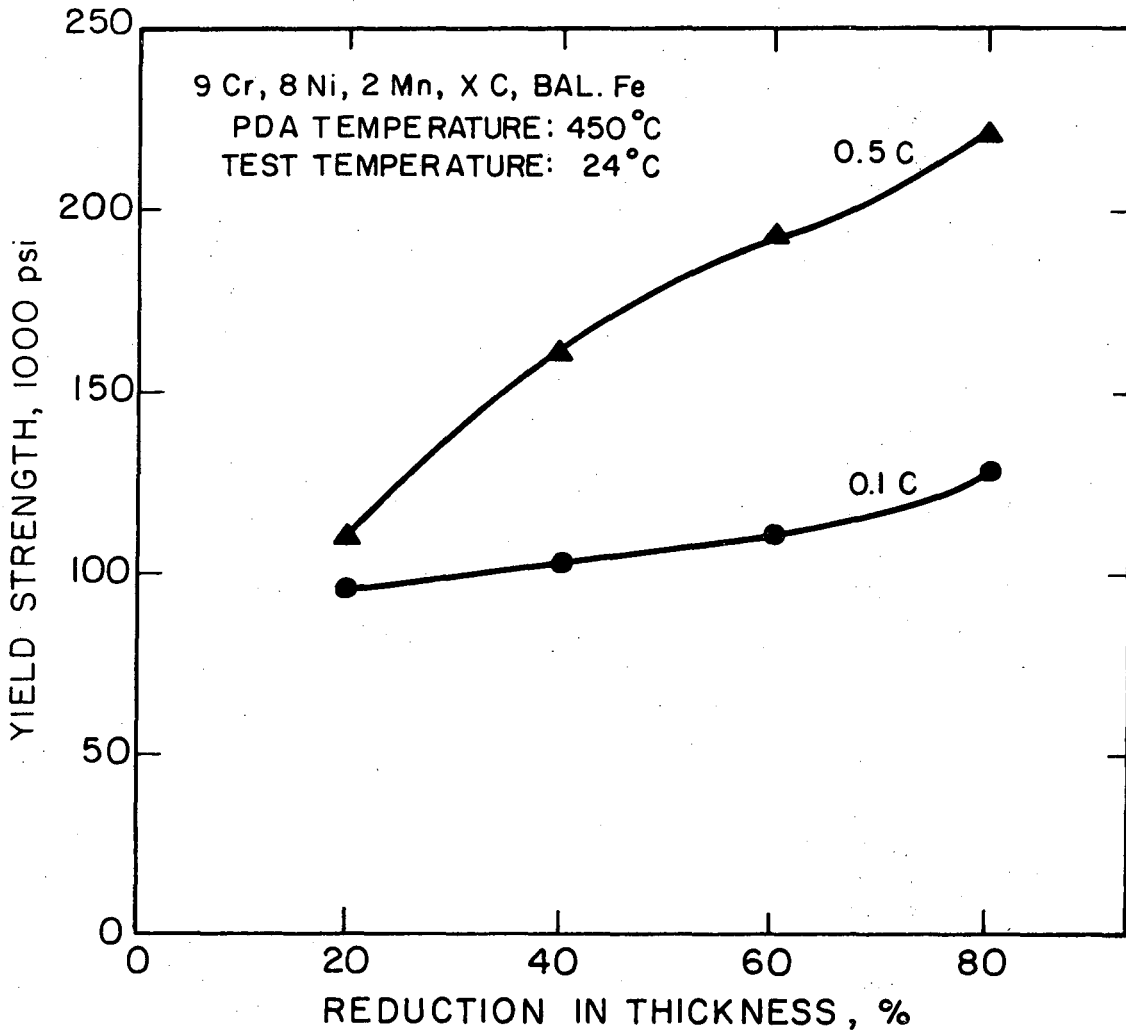
XBL 7110-7497

Fig. 7



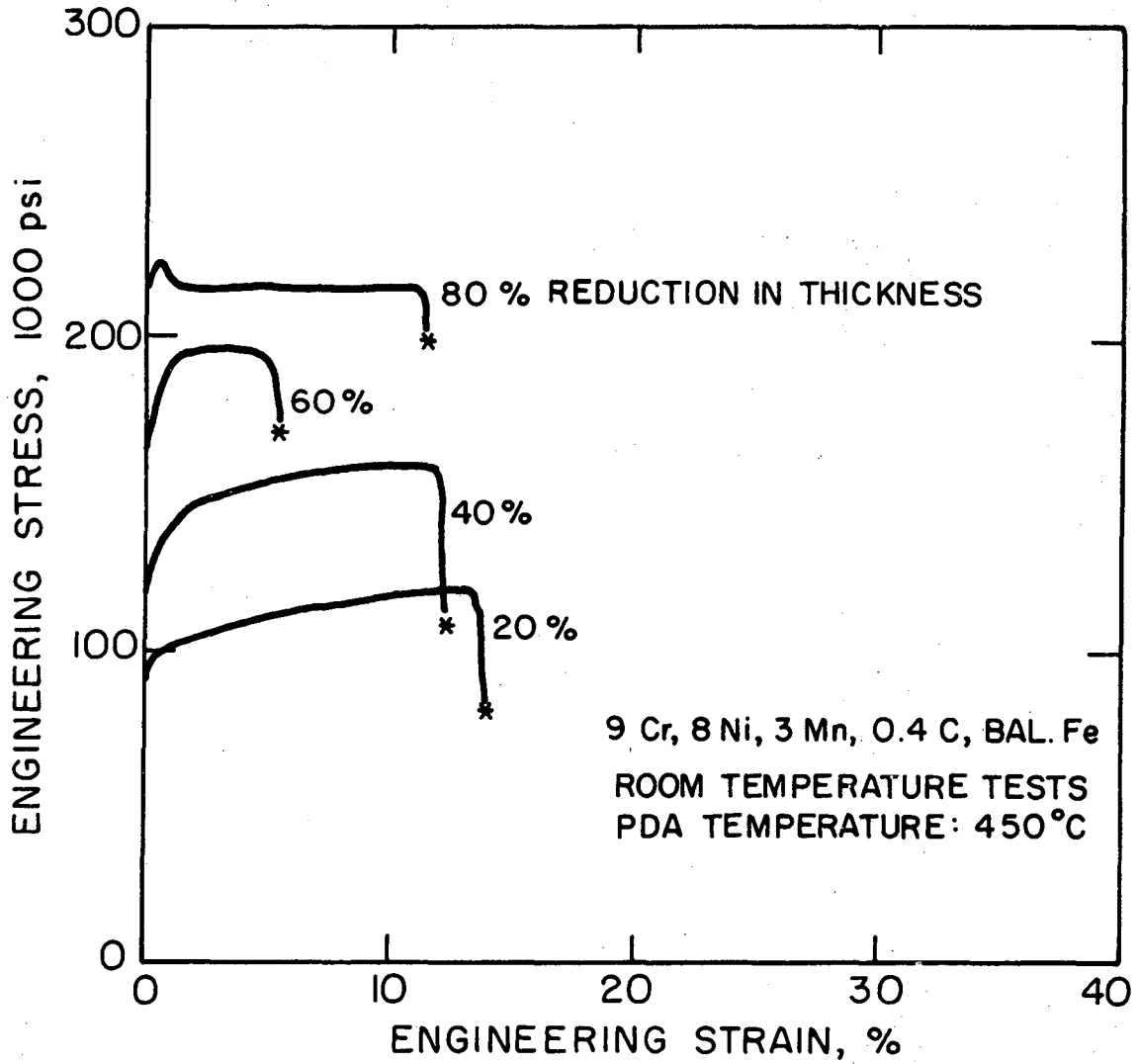
XBL 7110-7498

Fig. 8



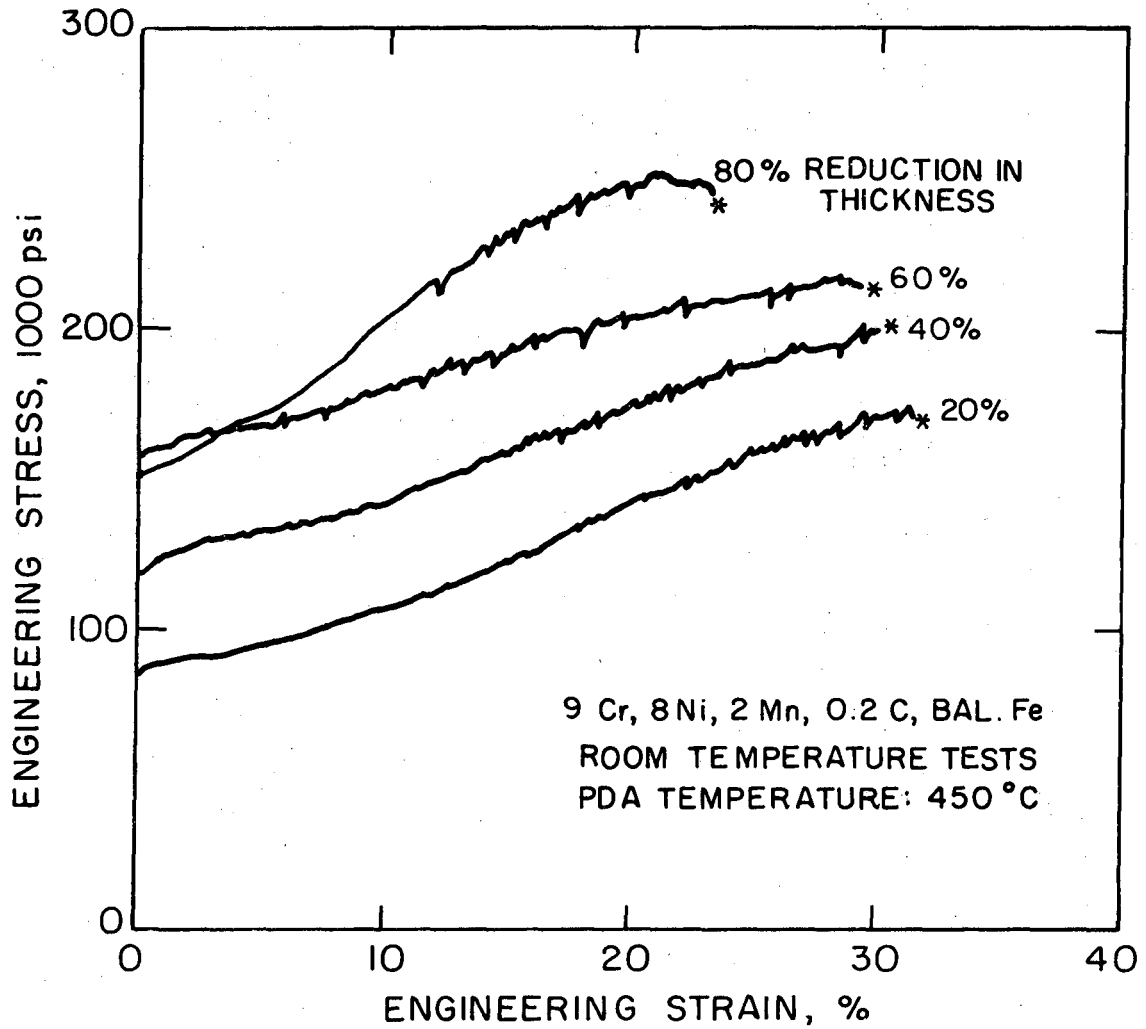
XBL 747-6827

Fig. 9



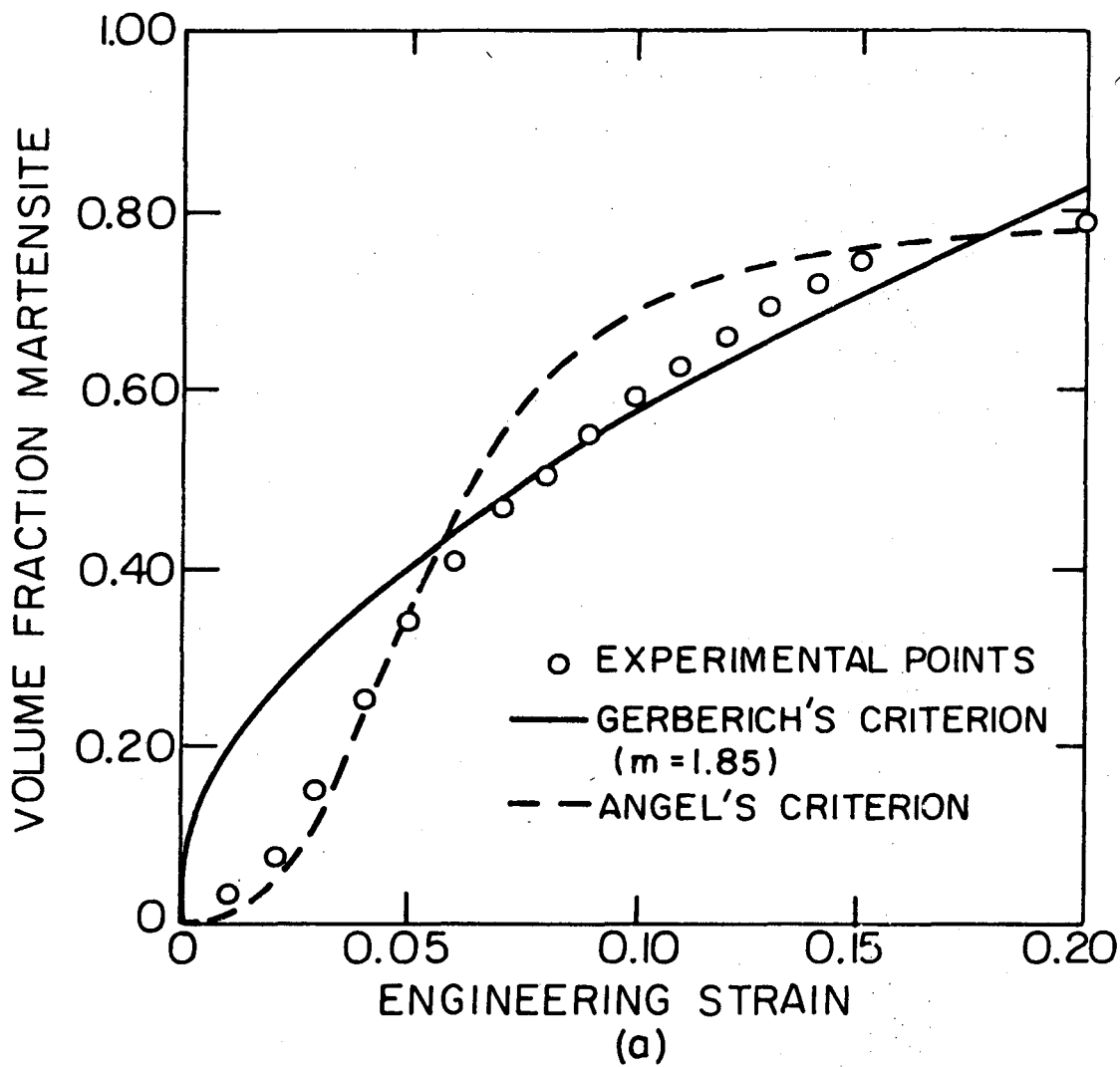
XBL 747- 6828

Fig. 10



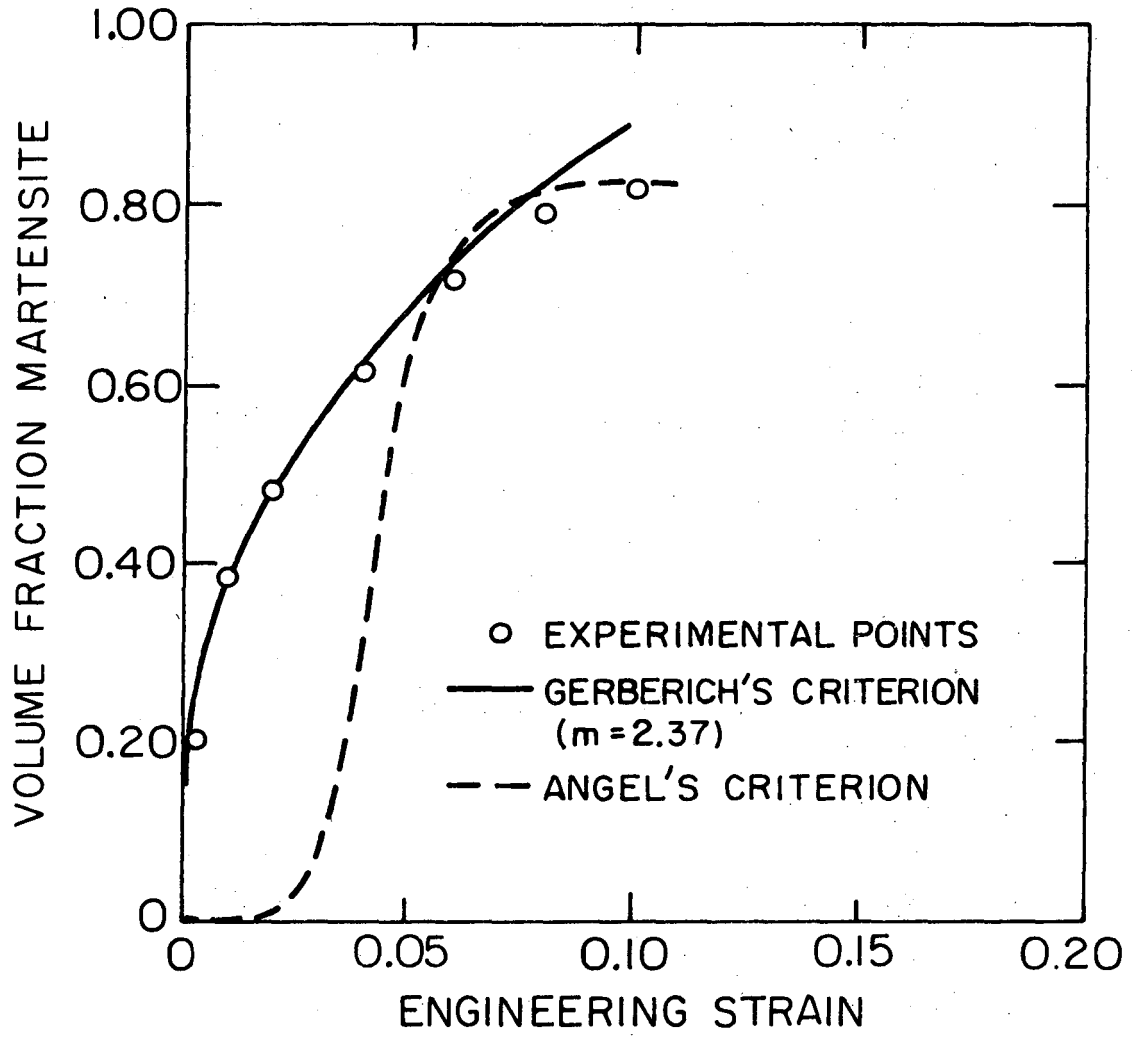
XBL 747-6829

Fig. 11



XBL 7110-7500

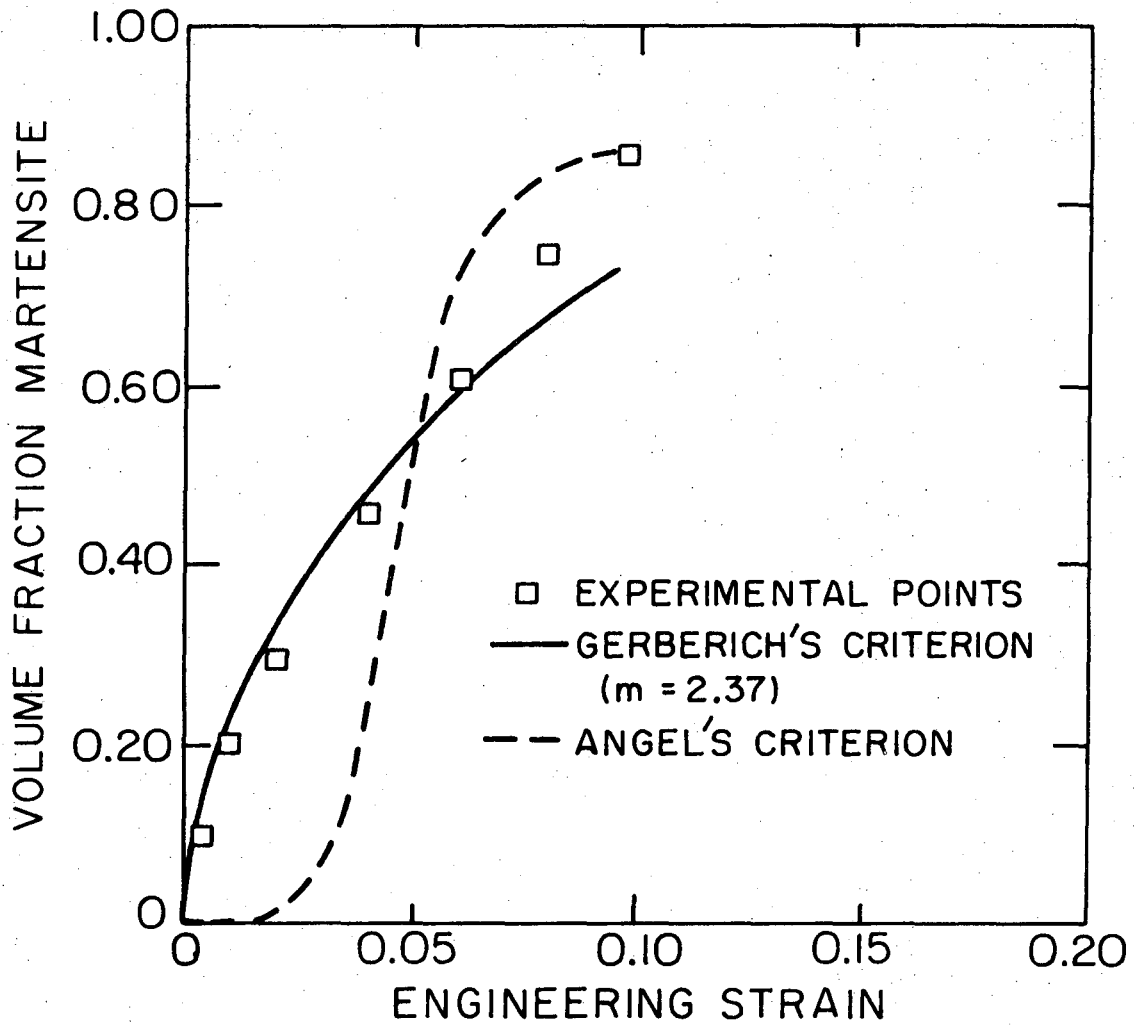
Fig. 12a



(b)

XBL 7110-7501

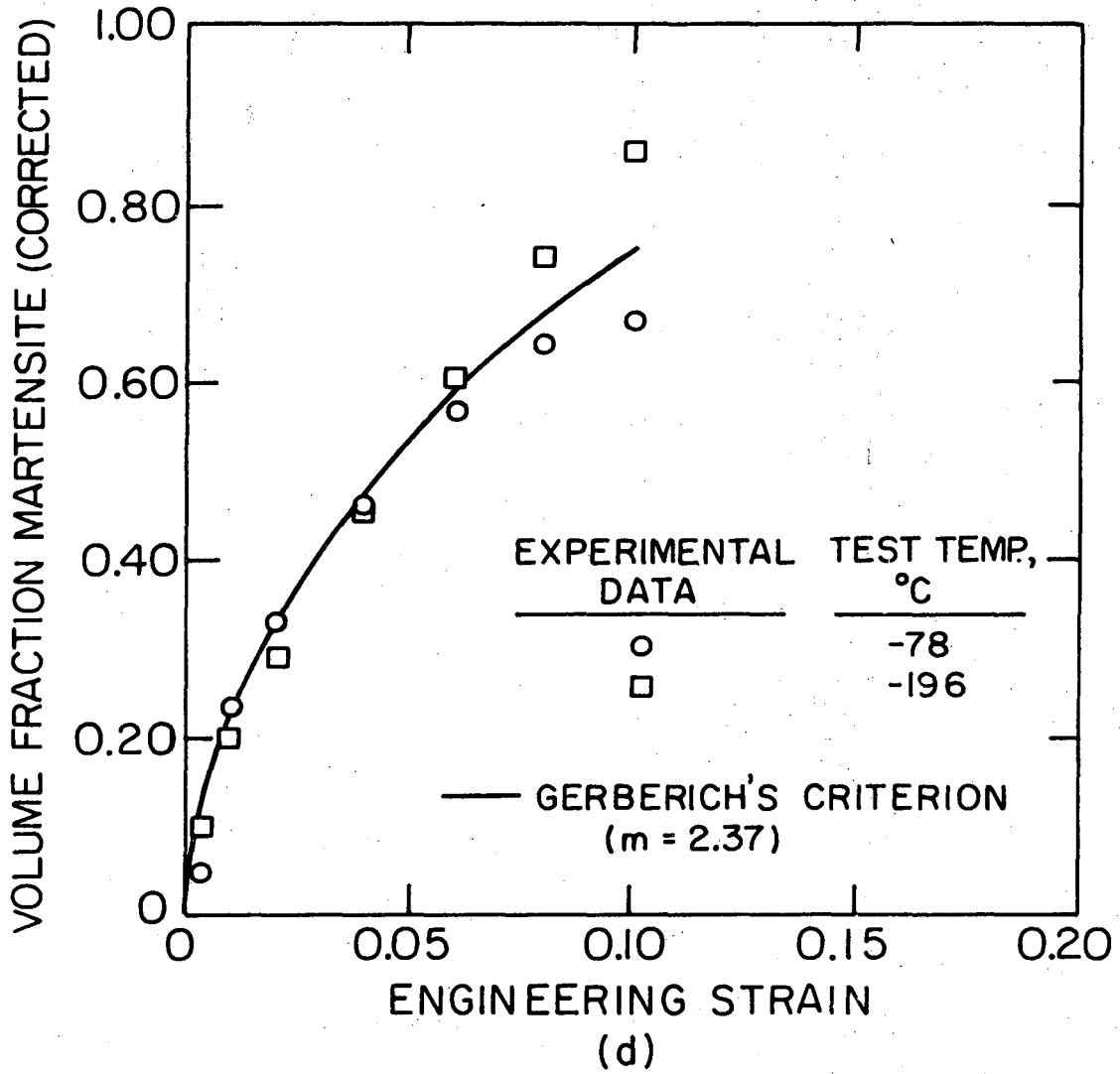
Fig. 12b



(c)

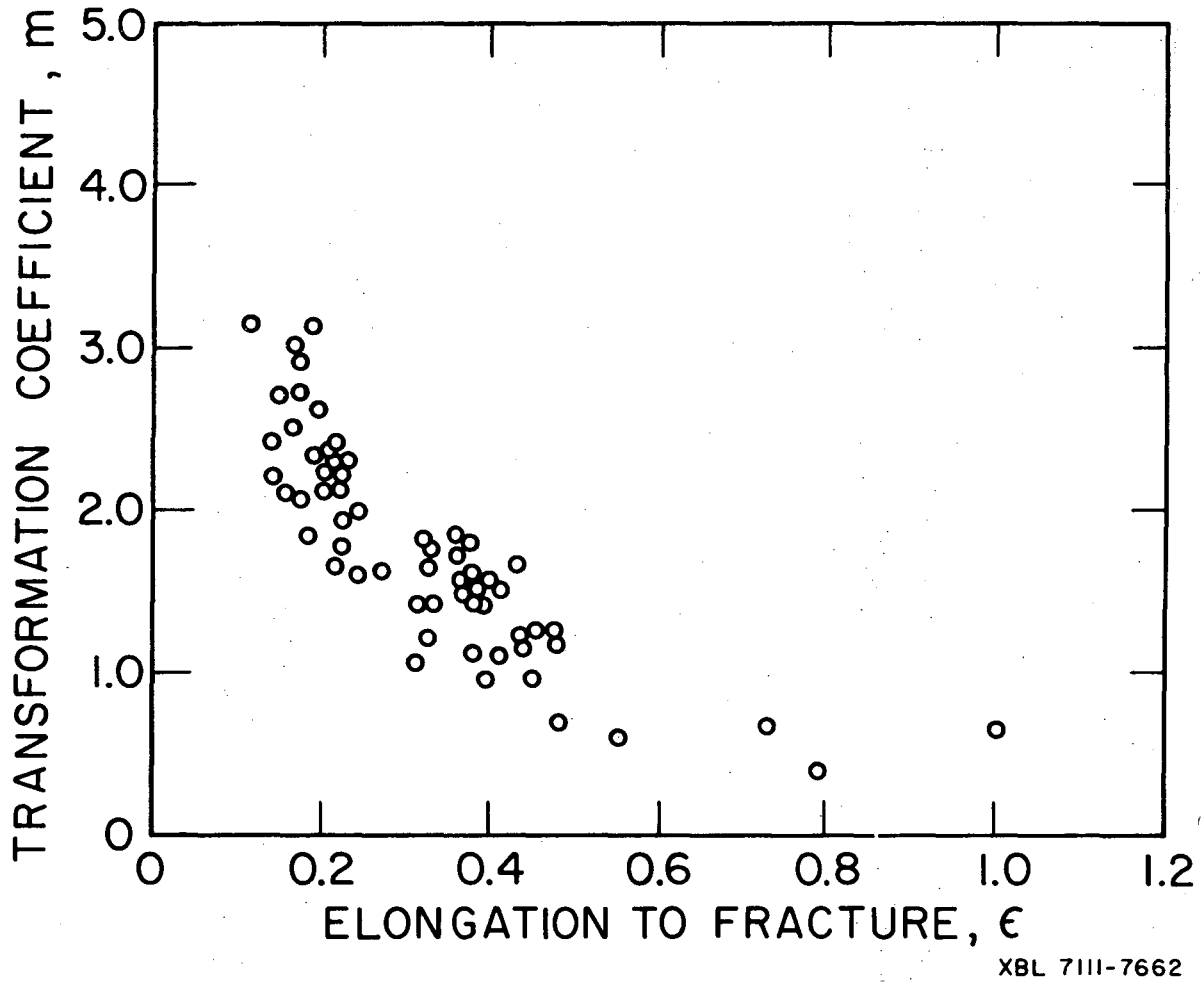
XBL 7110-7502

Fig. 12c



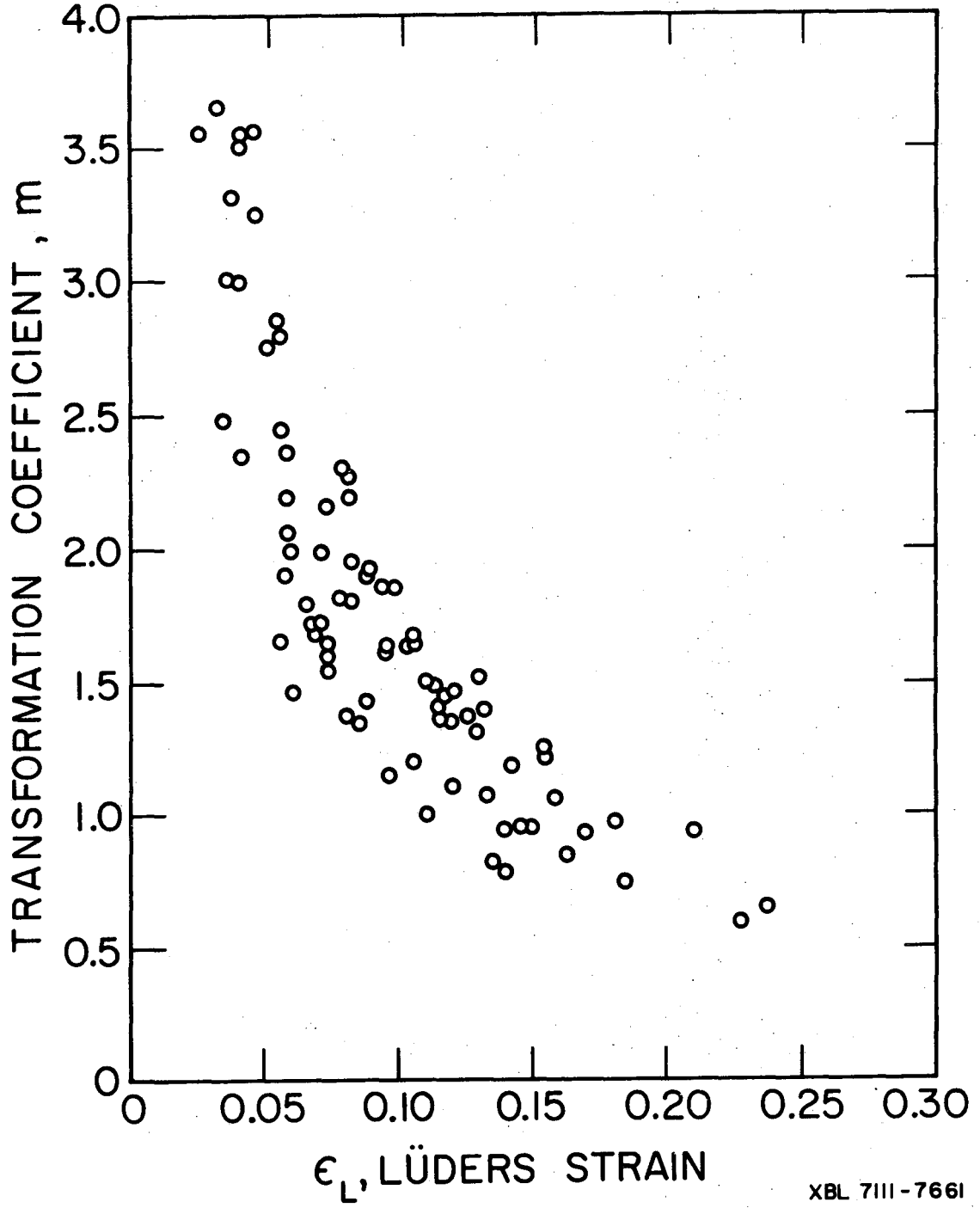
XBL 7110-7503

Fig. 12d



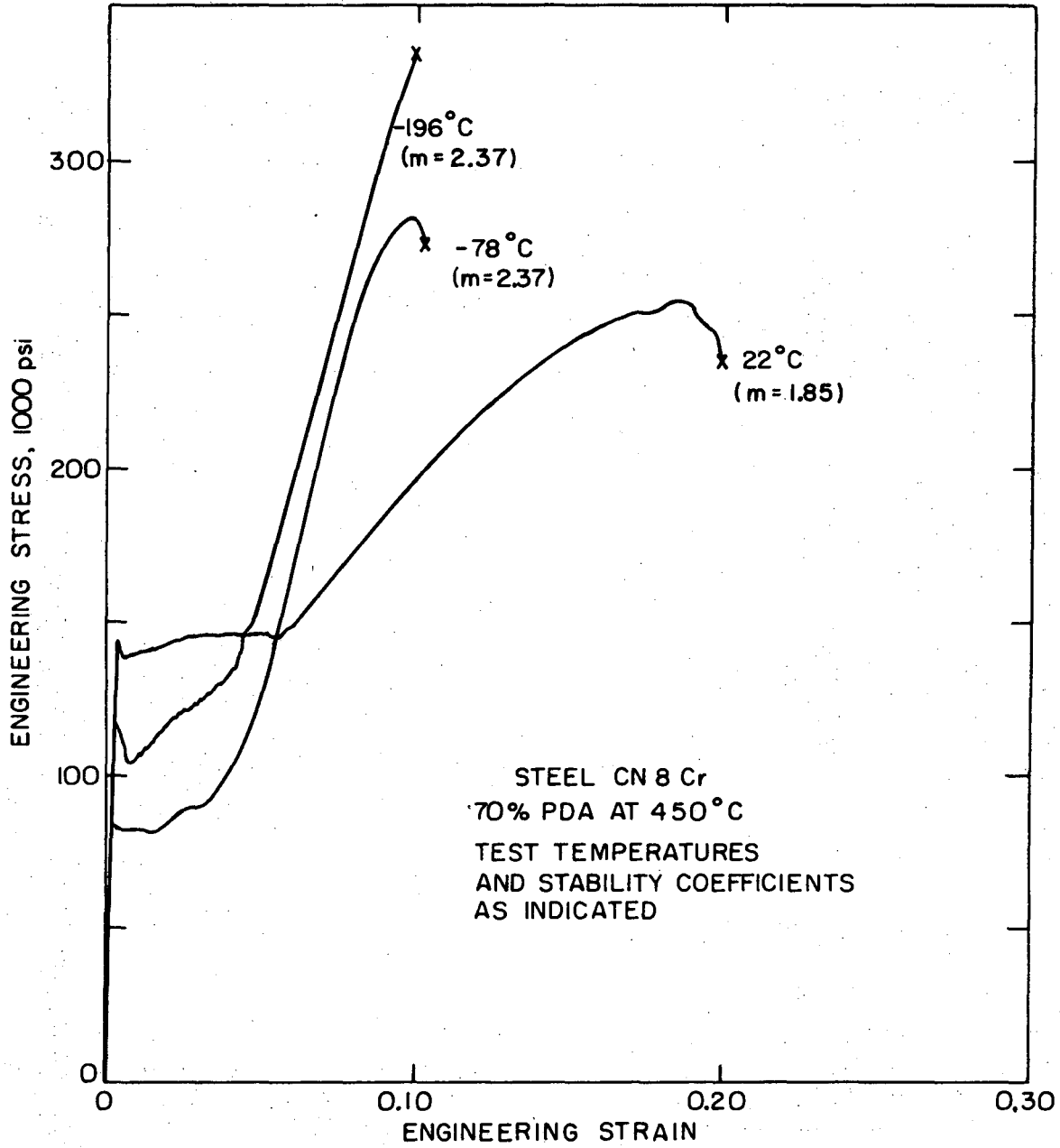
XBL 7111-7662

Fig. 13a



XBL 7111-7661

Fig. 13b



XBL 7110-7504

Fig. 14

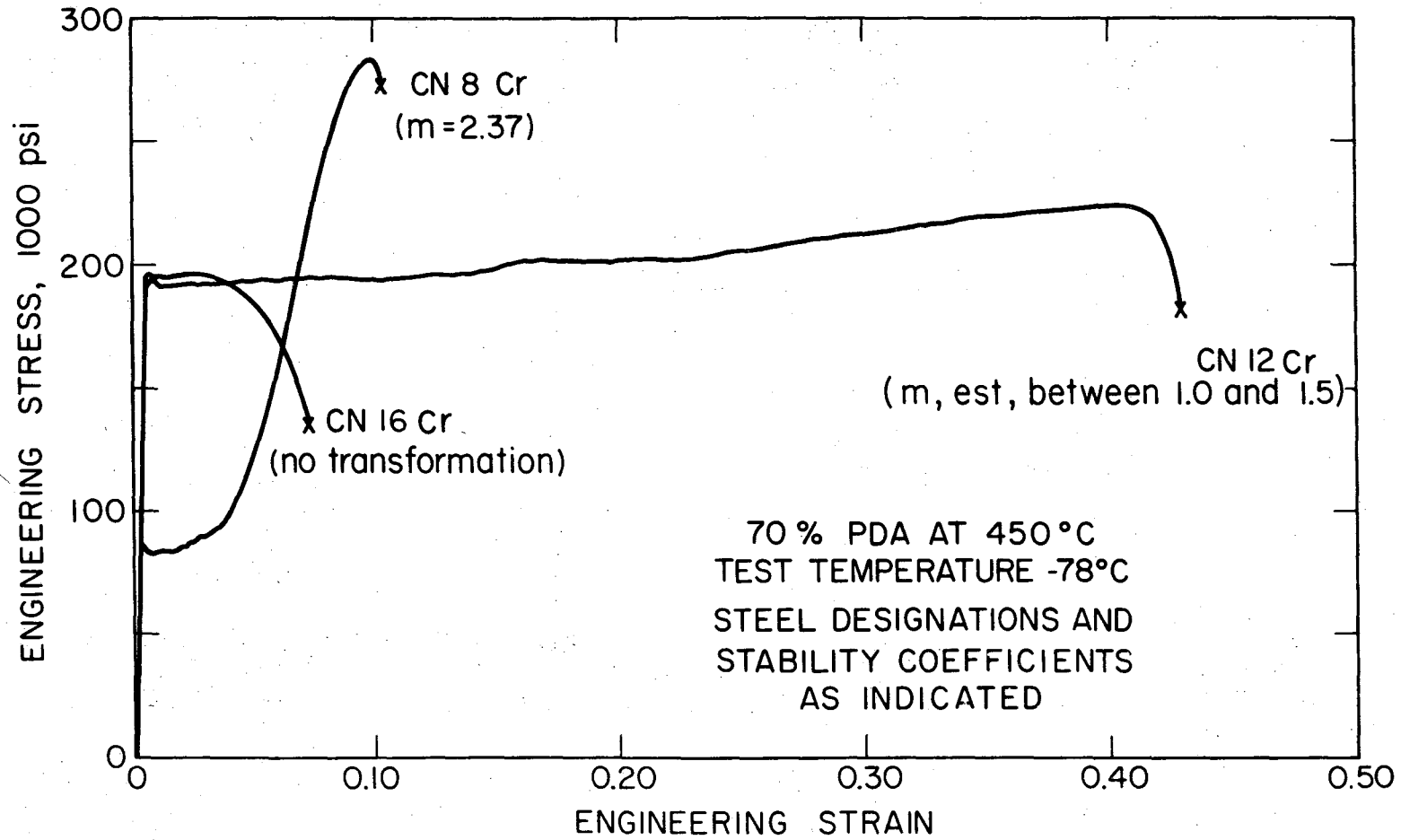
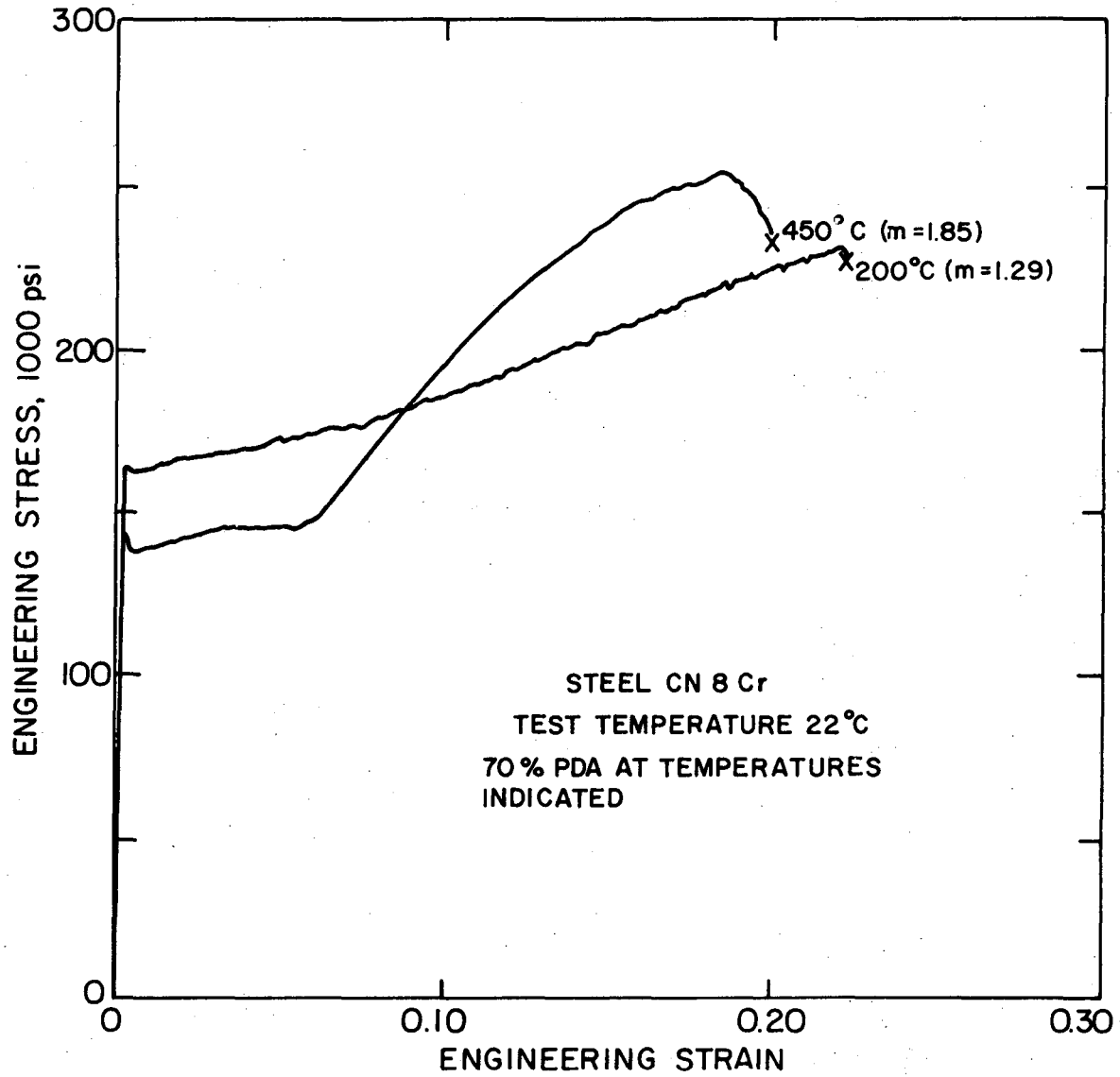
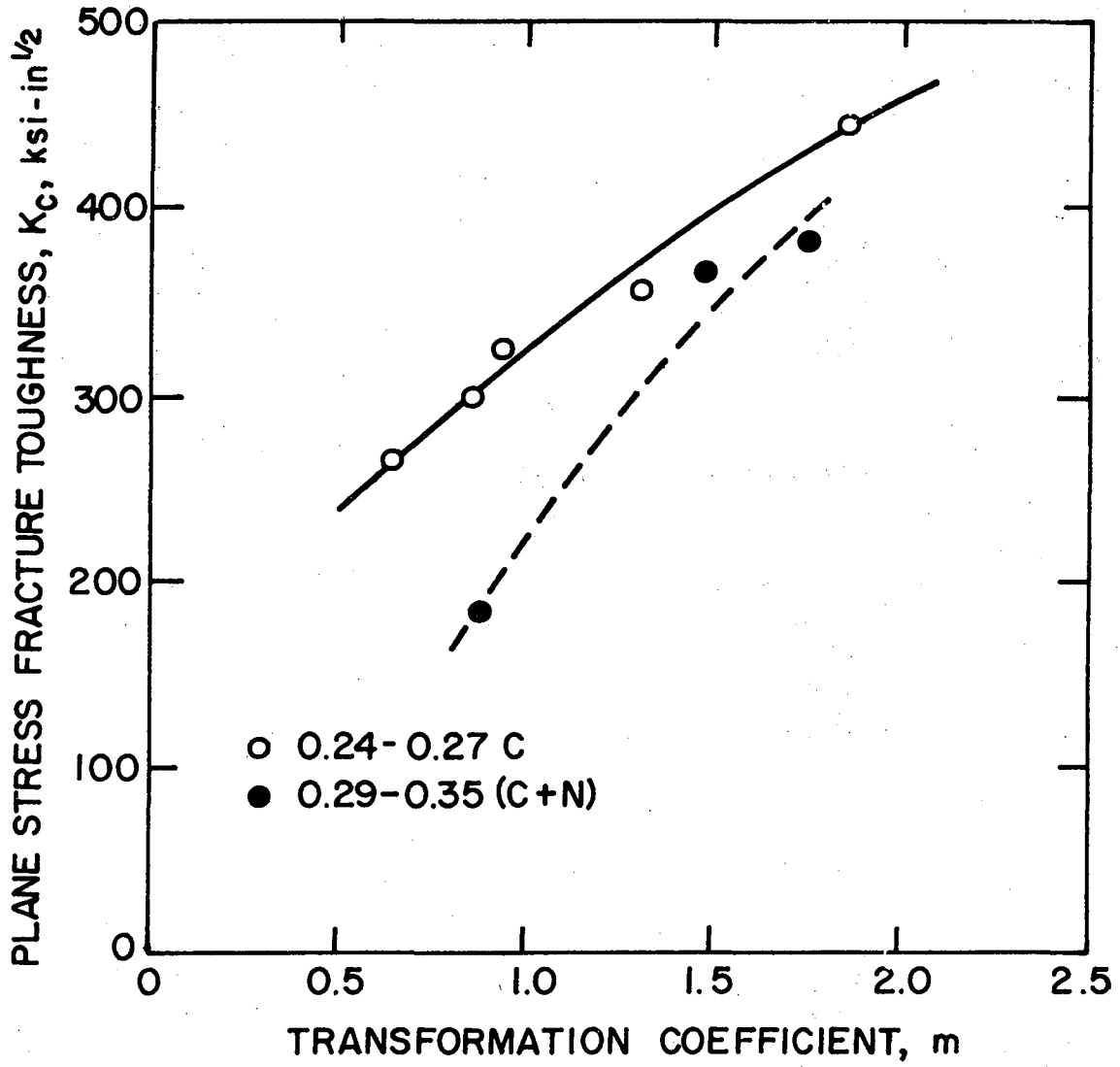


Fig. 15



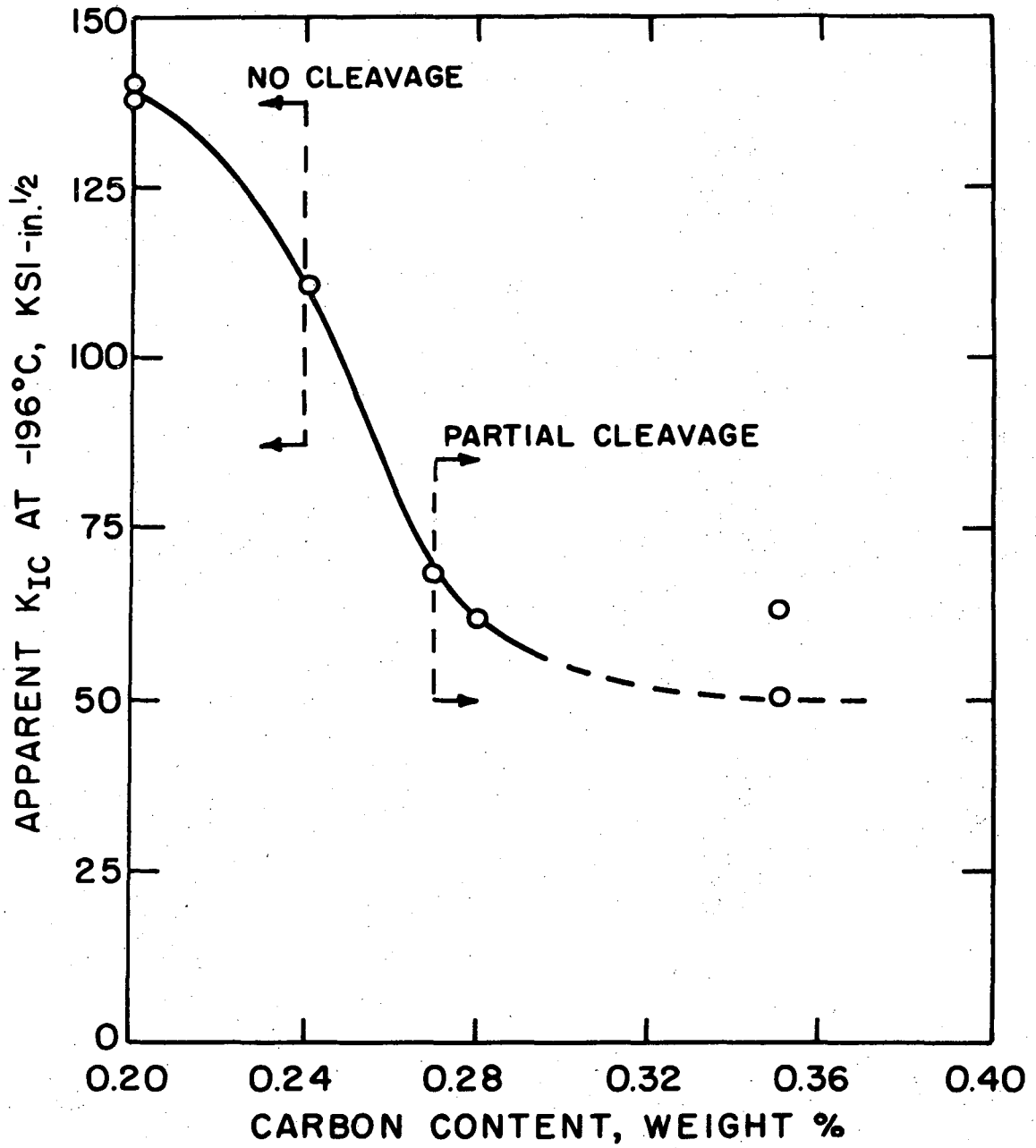
XBL 7110-7506 B

Fig. 16



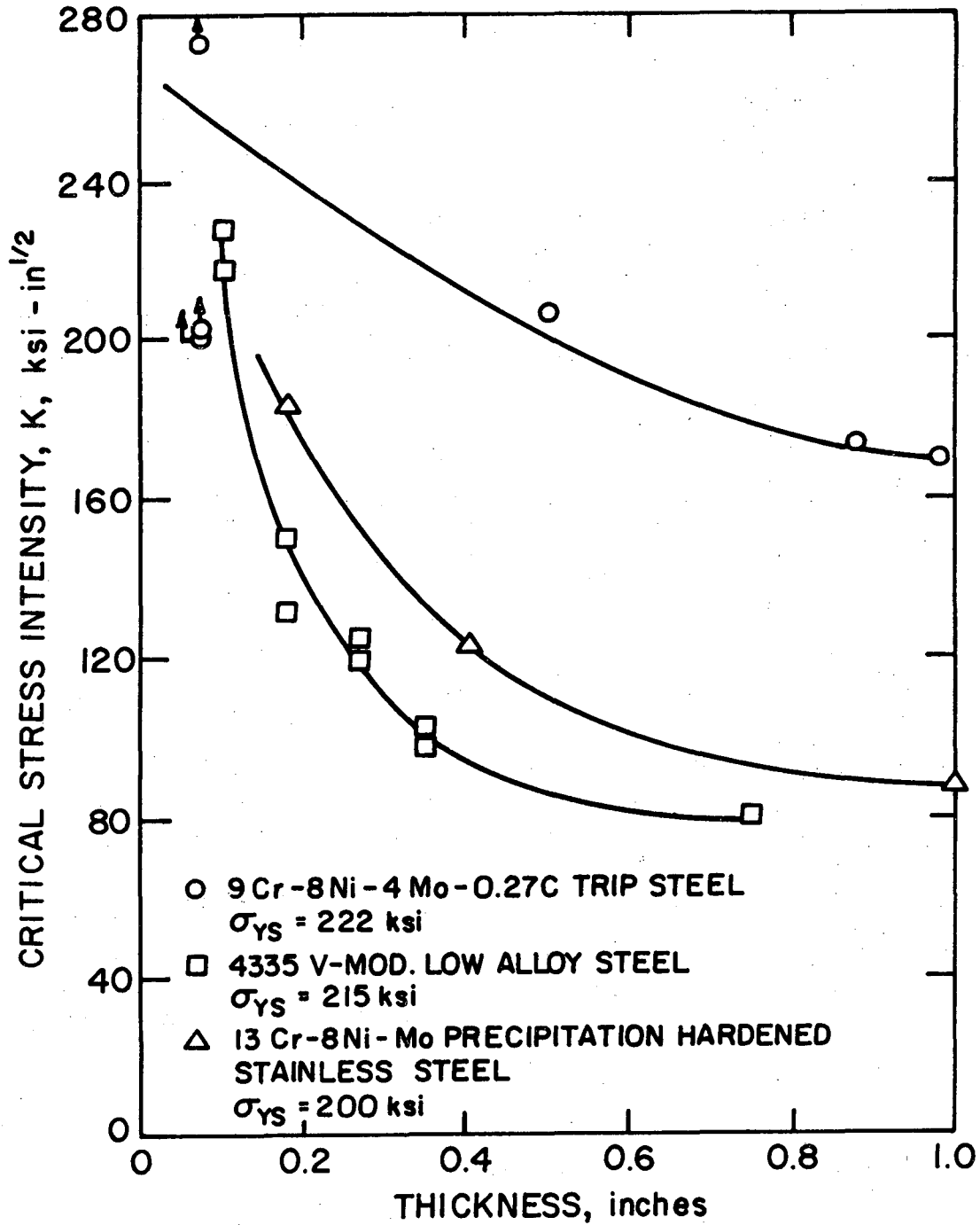
XBL 7011-6952 A

Fig. 17



XBL 701-210

Fig. 18



XBL6811-6156A

Fig. 19

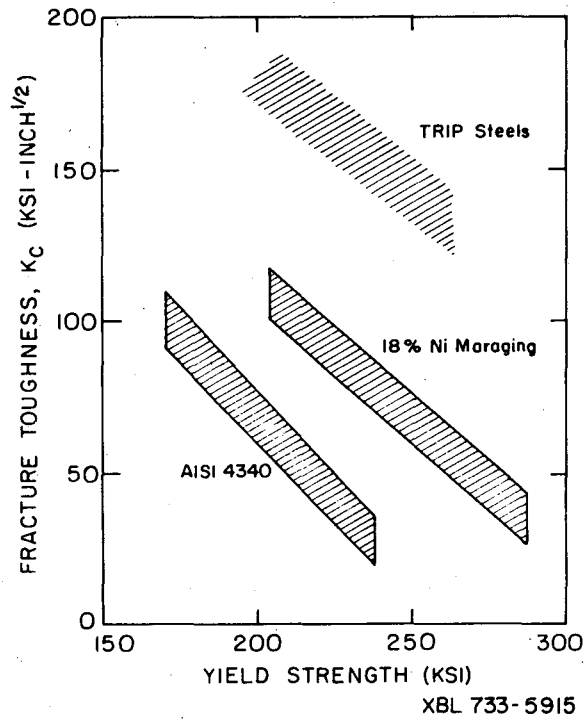


Fig. 20

LEGAL NOTICE

*This report was prepared as an account of work sponsored by the United States Government. Neither the United States nor the United States Atomic Energy Commission, nor any of their employees, nor any of their contractors, subcontractors, or their employees, makes any warranty, express or implied, or assumes any legal liability or responsibility for the accuracy, completeness or usefulness of any information, apparatus, product or process disclosed, or represents that its use would not infringe privately owned rights.*

TECHNICAL INFORMATION DIVISION  
LAWRENCE BERKELEY LABORATORY  
UNIVERSITY OF CALIFORNIA  
BERKELEY, CALIFORNIA 94720